DOI: 10.4408/IJEGE.2020-02.O-04

INFLUENCE OF GEOLOGICAL COMPLEXITIES ON LOCAL SEISMIC RESPONSE IN THE MUNICIPALITY OF FORIO (ISCHIA ISLAND, ITALY)

Salvatore MARTINO[(*,**)], Patrizia CAPRARI[(*,**)], Marta DELLA SETA[(*,**)], Carlo ESPOSITO[(*,**)], Matteo FIORUCCI[(*,**)], Salomon HAILEMIKAEL[(***)], Roberto IANNUCCI[(*,**)], Gian Marco MARMONI[(*,**)], Guido MARTINI[(***)], Antonella PACIELLO[(****)] & Alessandro PELOSO[(***)]

[(*)] *Sapienza University of Rome - Earth Sciences Department , P.le Aldo Moro n.5, I-00185 Rome, Italy*
[(**)] *CERI Research Centre - Sapienza University of Rome, P.le Aldo Moro n.5, I-00185 Rome, Italy*
[(***)] *ENEA National agency for new Technologies, energy and sustainable economic development - Frascati Research Center, Via Enrico Fermi n. 45, I-00044 Frascati, Rome, Italy*
[(****)] *ENEA National agency for new Technologies, energy and sustainable economic development - Casaccia Research Center, Via Anguillarese n. 301, I-00123, Santa Maria di Galeria, Rome, Italy*
Corresponding author: salvatore.martino@uniroma1.it

EXTENDED ABSTRACT

Le indagini geofisiche condotte nell'ambito degli studi di risposta sismica nel comune di Forio di Ischia a seguito del sisma del 21 Agosto 2017, hanno consentito di rilevare effetti locali connessi a specifiche condizioni dell'assetto geologico-strutturale che riflettono la complessità del contesto vulcanico che caratterizza l'intera isola di Ischia e, più nello specifico, il settore occidentale del Monte Epomeo e dell'adiacente piana costiera di Forio.

In particolare, tramite l'esecuzione di misure di rumore sismico ambientale a stazione singola, sono stati osservati: i) effetti di polarizzazione ed amplificazione in prossimità di elementi tettonici e sistemi di fratturazione che caratterizzano il promontorio di Zaro, dove affiorano depositi vulcanici da massivi a stratificati; ii) risonanze stratigrafiche su valori di frequenza apprezzabilmente variabili entro poche centinaia di metri, che possono essere messe in relazione alla giustapposizione di accumuli di frana (in particolare *debris*- e *rock-avalanches* o *lahars*) in corrispondenza dell'abitato di Forio, permettendone la corretta definizione spaziale; iii) amplificazione sismica, seppure in assenza di marcata polarizzazione del *ground motion*, nel settore di versante coinvolto nella deformazione gravitativa del Monte Nuovo e non apprezzabile nei settori adiacenti, che vedono affiorare le stesse unità litologiche coinvolte nella instabilità gravitativa.

Le peculiarità geologiche dei contesti analizzati ai fini della risposta sismica locale consentono di applicare differenti schemi interpretativi che variano dalla pura risonanza stratigrafica (modello monodimensionale di colonna risonante) perlopiù controllata da spessore e velocità di propagazione delle onde sismiche in depositi soffici su un substrato rigido, alla risonanza di corpi rocciosi fratturati non del tutto svincolati dall'adiacente substrato e per i quali non si raggiungono ancora condizioni di vibrazione libera con modi propri (modello tridimensionale di massa oscillante), fino alla combinazione di distribuzione della rigidezza nel sottosuolo e presenza di discontinuità fisiche in grado di polarizzare e amplificare lo scuotimento connesso alla propagazione delle onde di superficie.

Tali evidenze costituiscono una fondamentale chiave interpretativa per la zonazione sismica, proponendo l'individuazione di settori a comportamento ben definito ai quali attribuire schemi interpretativi della risposta sismica locale che non rientrano necessariamente nella codifica che distingue tra amplificazione stratigrafica o topografica prevista dalle attuali linee guida nazionali per gli studi di Microzonazione Sismica.

Ciò appare in linea con il recente approfondimento degli studi legato a diversi modelli di amplificazione sismica, nonché di modifica delle proprietà delle onde sismiche nel *near surface*, tra i quali: i) la presenza di sistemi rocciosi fratturati con marcate anisotropie che favoriscono la polarizzazione delle onde di superficie (Burjánek *et alii*, 2012); ii) la presenza di elementi rigidi disgiunti (quali blocchi di roccia) in grado di oscillare secondo modi propri amplificando e polarizzando le onde sismiche (Galea *et alii*, 2014; Iannucci *et alii*, 2018); iii) la presenza di morfologie di substrato o anche di depositi che focalizzano e polarizzano le onde di superficie (Panzera *et alii*, 2019); iv) la presenza di contatti laterali tra mezzi eterogenei che favoriscono l'intrappolamento delle onde sismiche con conseguente amplificazione e polarizzazione delle stesse (Pischiutta *et alii*, 2012).

Inoltre, per ciò che attiene le amplificazioni sismiche osservate in versanti instabili in roccia e connesse all'assetto stratigrafico e strutturale, di recente si sono affermati due schemi di risposta (Kleinbrod *et alii*, 2019; Martino *et alii,* 2020): un primo legato a spessori di materiale a forte contrasto di impedenza con il sottostante substrato e, pertanto, in grado di generare amplificazione dell'azione sismica in relazione al rapporto tra spessore e velocità di propagazione nel mezzo più deformabile (*depth-controlled condition*), un secondo legato alla mobilità di porzioni di terreno isolate dal circostante substrato grazie a discontinuità aperte e ben definite che manifestano la loro libertà cinematica (*volume-controlled condition*) attraverso l'oscillazione di volumi dalle forme peculiari a cui corrispondono modi propri di risonanza (*eigen modes*).

ABSTRACT

Seismic response studies carried out in the Municipality of Forio on Ischia (NA), southern Italy, following the 21st August 2017 earthquake allowed to detect local effects related to specific geological-structural settings that reflect the complexity of the volcanic context which characterises the entire island of Ischia and, more specifically, the western sector of Mt. Epomeo and the adjacent coastal plain of Forio.

In particular, the following features have been observed: i) polarization and amplification effects in the proximity of tectonic elements that dissect the Zaro promontory, where volcanic deposits from massive to stratified widely outcrop; ii) stratigraphic resonances on significantly variable frequency values, changing within distances of a few hundred meters, which can be related to the juxtaposition of landslide debris (such as debris-/rock-avalanches and lahar) in correspondence with the town of Forio; iii) seismic amplification in the sector involved in the ongoing gravitational deformation of Mt. Nuovo even in the absence of polarization of the particle motion.

The peculiarities of the geological contexts analysed in the Forio Municipality allow to apply different interpretative schemes that vary from stratigraphic resonance (one-dimensional model of resonant column) mostly controlled by thickness and wave velocity in soft soils onto a stiff bedrock, to the resonance of jointed rock masses which are not completely released from the adjacent bedrock so avoiding typical free vibrations with normal modes (three-dimensional oscillating mass model), or to the interaction in the near surface with physical discontinuities responsible for modifying the physical properties of surface waves polarizing and amplifying them.

The collected evidence of local seismic response in Forio exemplifies how not conventional interpretative keys for seismic zoning can be proposed to identify sectors whose response schemes do not necessarily fall within the standard of stratigraphic or topographical amplification adopted by current national guidelines for Seismic Microzonation (SM) studies. In particular, the evidence of local seismic response collected for the Forio Municipality were taken into account in the SM and relative products that were realised in the following years.

***Keywords**: Seismic microzonation, local seismic response, engineering-geological model, Island of Ischia*

INTRODUCTION

Since a decade, Seismic Microzonation (SM) studies in Italy are a tool of substantial support for environmental planning in the management of seismic risk. Guidelines for SM, proposed by the Italian Department of Civil Protection (ICMS Working Group, 2008) following Regional Decrees that have defined standards and techniques, aim at identifying amplification conditions and instabilities induced by the expected seismic action. The Italian National guidelines for SM studies define a three-level methodology including a level - 1 qualitative approach which restitutes a preliminary mapping of homogeneous zones expected in terms of local seismic response (namely the MOPS map); a semi-quantitative second level analyses where amplification factors referred to seismic microzones are computed based on simplified approaches; a third quantitative level, based on analysis including numerical modelling and analytical computation of amplification factors referred to the identified seismic microzones.

Far beyond a possible standardisation, the local seismic response studies presuppose an engineering-geological modelling of the subsoil such as to support interpretive response models, which make use of instrumental techniques (geophysical investigations) and numerical analysis (mono-, two- or three-dimensional). The geological complexities of the subsoil, therefore, play a fundamental role in the interpretation of the effects of local seismic response which can be ascribed to processes often very different from stratigraphic amplification, i.e., from the vertical juxtaposition of deposits with sufficiently different seismic impedances.

In this sense, in the last decades several models of seismic amplification as well as modification of the seismic waves properties in the near surface have been studied, among these: i) the presence of jointed rock masses with marked anisotropies that favour the polarization of surface waves (Burjánek *et alii,* 2012 and references therein); ii) the presence of disjoint rigid elements (such as rock blocks) which can oscillate according to their own vibrational modes, causing amplification and polarization of the propagating seismic waves (Galea *et alii,* 2014; Iannucci *et alii,* 2018 and references therein); iii) bedrock shapes or soil geometries that focus and polarize surface waves, resulting in a marked zoning of their effects (Panzera *et alii*, 2019 and references therein); iv) the presence of lateral contacts between heterogeneous media which favour the entrapment of seismic waves with consequent amplification and polarization (Pischiutta *et alii*, 2012 and references therein).

As it regards the seismic amplifications observed in unstable rock slopes and related to the stratigraphic and structural setting, two response schemes have been very recently proposed (Kleinbrod *et alii,* 2019): a first one linked to deposits having a strong impedance contrast with the underlying substrate and therefore able to generate an amplification of the seismic action mostly connected to the relationship between thickness and seismic wave speed in the most deformable medium (depth controlled condition); a second one linked to the mobility of portions of subsoil isolated from the surrounding by open and well-defined discontinuities (volume controlled condition) through the oscillation of volumes with peculiar shapes to

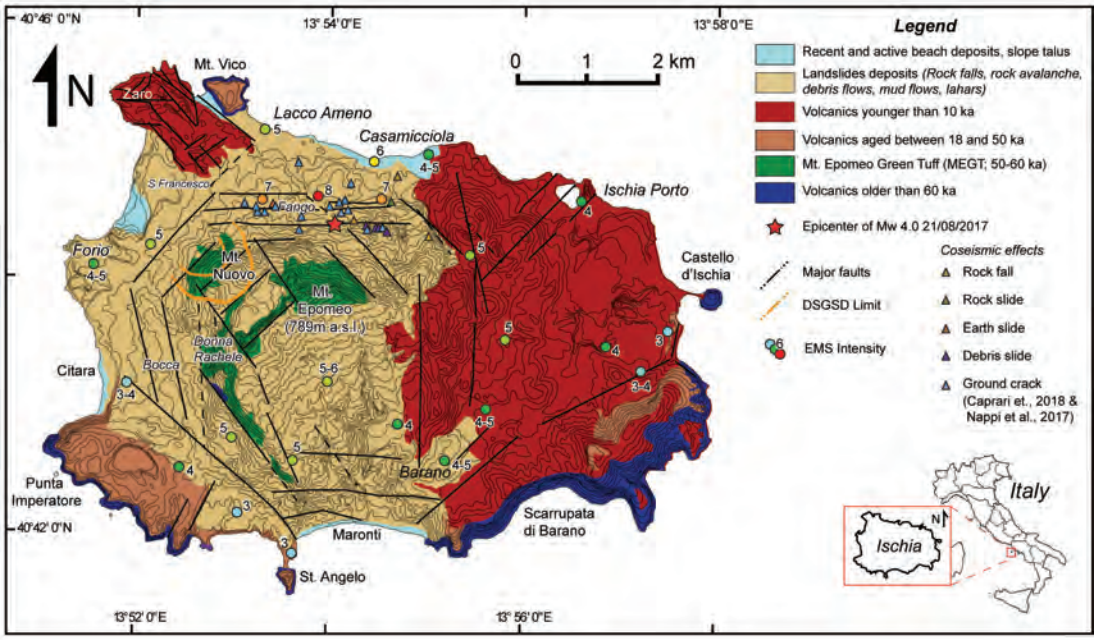

Fig. 1 - Geological sketch of the island of Ischia (NA). The epicentre of the 21st August 2017 earthquake, the EMS intensities and the earthquake-induced effects (from the CEDIT catalogue - http://www.ceri.uniroma1.it/index.php/web-gis/cedit/) are also reported

which correspond resonance modes (*eigen modes*).

The complexities of some geological contexts sometimes add to the aforementioned conditions predisposing the local seismic response, other times they fade their specificity, leading to local seismic response models attributable to less defined schemes and as such less generalizable (Martino *et alii,* 2020).

The here considered case study results from research activities carried out in the municipal area of Forio on the island of Ischia (NA), southern Italy (Fig. 1), on behalf of the Department of Civil Protection through the Seismic Microzonation Centre and its Applications of Italian National Research Council, in application of the Resolution of the Council of Ministers of 29/08/2017 issued following the 21st August 2017 M_w 4.0 Casamicciola (NA) earthquake (epicentre coordinates 40°44′24″N; 13°54′00″E) that struck the northern sector of the island (Fig. 1) and the Casamicciola municipality in which damage was surveyed up to a 8th level on the EMS scale (Azzaro *et alii*, 2017). The same area was already struck by the dramatic event of the 28th July 1883, that widely damaged buildings in the North and Western sectors of the Island (MCS IX-X) and caused more than 2300 fatalities (Guidoboni *et alii*, 2007).

In this research, the main outcomes resulting from local seismic response studies propaedeutic to SM carried out in the municipal area of Forio were reported. The area is characterised by a marked variability of geological contexts linked to the volcano-tectonic and morphostructural evolution of the western sector of the island which results from a peculiar calderic resurgence caldera. Some peculiar conditions of the local geology represent the interpretative key of seismic amplification effects detectable through instrumental investigations that are the main topic of this study.

GEOLOGICAL FEATURES

The island of Ischia (Fig. 1) represents the westernmost part of the Phlegraean Volcanic District (Central Italy) and its formation is the direct expression of volcanic activity related to the opening of the Tyrrhenian margin of the Apennine chain (Orsi *et alii,* 2003).

The current geological and morphological framework of the island is the result of one of the most spectacular cases of caldera resurgence in the World, which actively and passively conditions the local morphostructural and geostructural setting and, in general, its recent evolution.

Volcanic activity on Ischia island began prior to 150 ka (Rittmann, 1930; Vezzoli, 1988; Sbrana & Toccaceli, 2011) and continued until the beginning of the 14th century with small volume events characterised by effusive and sporadic explosive magmatic and hydro-magmatic style eruptions (as last the Arso lava flow in 1302 - Vezzoli, 1988; De Vita *et alii,* 2010). The main event that marks the geological history of the island was dated 55 ka, when a major explosive eruption (40 km^3 in volume - Tomlinson *et alii,* 2014) led to the caldera formation and the emplacement of a massive greenish alkali-trachytic pyroclastic

flow deposit named Mt. Epomeo Green Tuff (MEGT - Orsi *et alii*, 1991; Tibaldi & Vezzoli, 1998; Brown *et alii*, 2008).

The collapse of the caldera was followed by the asymmetric and structurally-controlled resurgence of the Mt. Epomeo block, which was lifted up of about 900 m in the last 28-33 ka BP with an intermittent style (Tibaldi & Vezzoli, 1998; Molin *et alii*, 2003). The resurgence isolated polygonal shape blocks that were differentially displaced and tilted, as clearly visible in satellite or aerial photos.

The resurgence has been driven by an increase in volume or pressurisation of the shallow magmatic systems (Orsi *et alii*, 1991; Tibaldi & Vezzoli, 1998).

The magmatic body also causes the presence of a vapour dominated hydrothermal system characterised by high heat fluxes (200-400 mW/m^2 - Carlino *et alii*, 2014).

The principal surficial evidence of the presence of vigorous hydrothermal circulation are several thermal springs and fumaroles with temperature up to 100°C, among which, the most vigorous are localised in the western sector of the island.

As other volcanic island worldwide, Ischia was also the best setting for slope instabilities: the island host several processes at different scales and experienced, since the Holocene, events ranging from shallow mass movements up to massive rock slope failures, whose location and temporal occurrence attest their close connection with volcano-tectonic activity (Tibaldi & Vezzoli, 2004; De Vita *et alii*, 2006; Della Seta *et alii*, 2012).

The most unstable slopes are located to the northwest of Mt. Epomeo, where large debris avalanches detached from the edge of the resurgent block, as documented by their huge deposits outcropping in the Forio Municipality coastal plain (Della Seta *et alii*, 2012; Sansivero *et alii*, 2018).

In addition to these large landslides, which represent the major catastrophic mass movements occurred in the island, a still active Mass Rock Creep (MRC) process takes place in the western sector of the island in Mt. Nuovo area, westward and downslope the Mt. Epomeo relief (Della Seta *et alii*, 2015; Marmoni *et alii*, 2017a).

The recent evolution of the geological processes affecting the island of Ischia presently predispose to multihazard conditions and related multirisk scenarios (Selva *et alii*., 2019) which include volcanism, seismicity, gravity-induced slope deformations, geothermal activity and the related chain effects such as debris avalanches/flows, earthquake-induced landslides and tsunami.

The clearest evidences of the old and recent volcanic activity experienced by the island, as well as its geomorphological evolution, both for large landslides (debris- and rock-avalanches, lahar) and ongoing slope-scale deformative process, are visible in the Forio Municipality.

In the following, based on peculiar geological features,

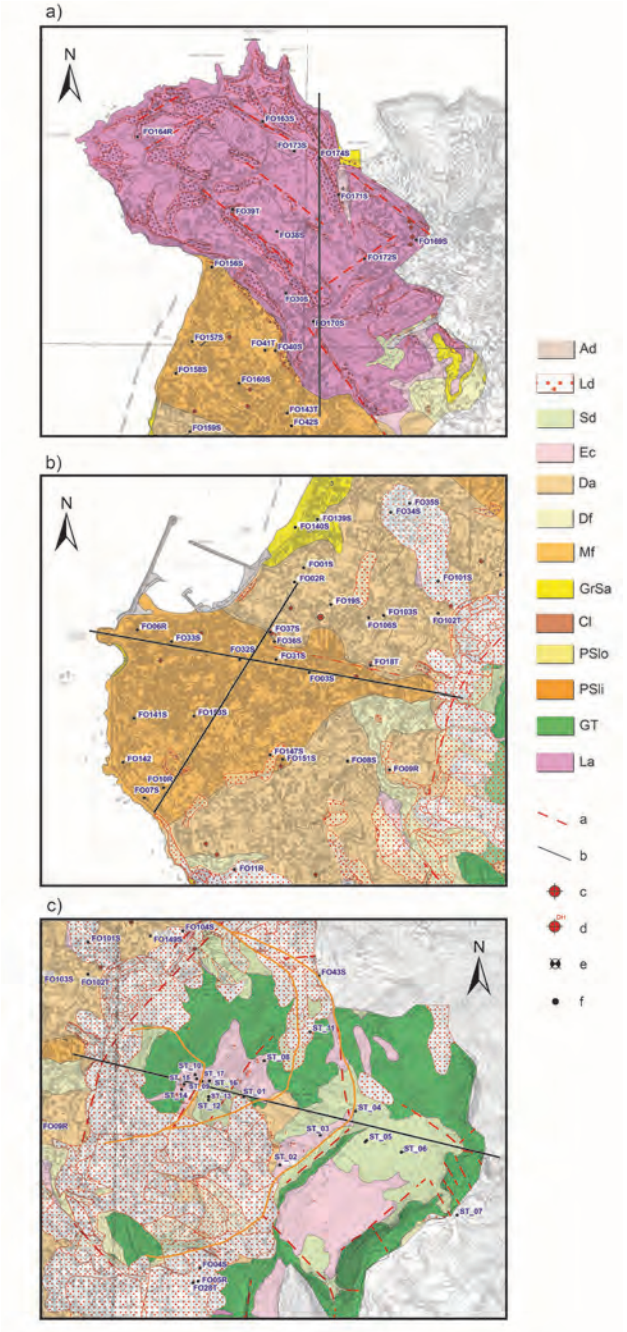

Fig. 2 - Geological sketch maps of the selected case studies in the island of Ischia (NA): a) Zaro promontory; b) Forio lahars; c) Mt. Nuovo deforming slope. Legend: ***Ad*** *-Man-made fill,* ***Ld*** *- Landslide deposit; Sd - slope debris;* ***Da*** *- Debris avalanche;* ***Df*** *- Debris flow and alluvial deposit;* ***Mf*** *- Lahar (mud flows);* ***GrSa*** *- Sandy gravels and coarse marine sands, sands;* ***Cl*** *- Clays;* ***PSlo*** *- Stratified loose pyroclastic deposit;* ***GT*** *- Massive and lithoid tuffs;* ***La*** *- Lavas;* ***a*** *- Faults;* ***b*** *- Trace of section;* ***c*** *- Borehole;* ***d*** *- Down-hole;* ***e*** *- Deep Borehole (Geothermal Exploration);* ***f*** *– Single-station seismic ambient noise measurement*

three distinctive sectors were identified and a brief description is provided for an accurate interpretation of the local seismic response in view of SM studies.

In particular, the above-mentioned sectors were identified in:

i) the Zaro promontory, representative of the recent lavic volcanics with diffused evidence of cracking and faulting;
ii) the Forio plain where recent volcaniclastic gravitational deposits are exemplified by a lahar outcropping in the coastal plain with a well-defined geometry, changing in width and thickness moving both from apical to distal areas and laterally;
iii) the Mt. Nuovo hills relief, in the westernmost sector of Mt. Epomeo, where a slope-scale gravity-induced deformation is affecting the rock mass with diffused evidence of trenches and scarps.

Zaro promontory

The Zaro promontory (Fig. 2a) constitutes one of the volcanic centres located along the caldera rim that erupted in the last stage of activity of the Ischia island, which began 10 ka BP. The Zaro centre of emission represents one of the 46 eruptive vents recognised in the period 3.000 ka BP-1302 A.D. (De Vita *et alii,* 2010, 2013). The emplacement of viscous trachytic lava flows and domes was driven by N45E- and N50W-trending fractures (De Vita *et alii*, 2010) featured by a discontinuous occurrence, reflecting the intermittent reprise of the volcano-tectonic activity and resurgence (Tibaldi & Vezzoli, 1998; De Vita *et alii*, 2006).

In the area, the thick lavas, previously interpreted as a single lava flow, are retained as emplaced by several lava domes and flows erupted since 6 +- 2.2 ka in a short time span (De Vita *et al.*, 2010) over an unattributed pyroclastic sequence older than 10 ka possibly related to Citara tuff sequence.They are constituted by 100-m-thick, light gray in color, porphyritic black trachytic lavas (Sbrana & Toccaceli, 2011).

Forio lahars

The coastal plain of Forio is widespreadly covered by rock avalanche deposits and debris and rockslides deposits. Single bodies of slope failure have been mapped in this sector of the island by Della Seta *et alii* (2012) based on geomorphological, stratigraphic and textural analyses which allowed to reconstruct ante-quem and post-quem relative datations.

The largest events are constituted by large rock- and debris avalanches (whose basal contact outcrops along the coast in Pietre Rosse) related to collapses of the volcanic resurgent slope, that detached from the hydrothermally altered and fractured rock mass. Such deposits, nowadays visible in the whole lowlands, are marked by typical linear ridges, levees and embedded blocks that feature a hummocky topography (Fig. 2b).

Above them, large and small lahars as well as minor mass movements such as rock falls, slumps and debris slides, buried the large avalanches, and above and around them developed the urban area Forio.

Elongated and lobate deposits extend from the foot of Mt. Epomeo relief towards the sea laying on the top of debris avalanche deposits. The clearest feature, interpreted by Della Seta *et alii* (2012) as lahar deposits, outcrops in Forio from the San Francesco shore to the Citara Bay, south of the local harbour.

A main lahar body characterised by massive and chaotic structure made up of a lithified greenish-grey matrix was outlined in the area of Forio, where it is superimposed over a coarser matrix and block supported avalanche deposits. In this study, the peculiarities of volcaniclastic deposits in terms of seismic site response is pointed out, reconstructing geometries and behaviour by means of the available boreholes and seismic ambient noise records.

Mt. Nuovo deforming slope

A remnant portion of the failed edge of Mt. Epomeo resurgent block is constituted by the Mt. Nuovo relief. The gravity-induced process affecting it covers an area of about 1.6 km^2 (Fig. 2c) involving a succession of alkali-trachyte pale green-coloured, welded ignimbrite units, characterised by very high porosity and poor litotechnical properties (Marmoni *et alii*, 2017a, 2017b; Heap *et alii*, 2018).

Based on a combination of engineering-geological and geomorphological field-surveys, terrain analyses and geophysical reconstructions, Della Seta *et alii* (2015) inferred a structurally controlled biplanar compound surface as the main mechanism controlling the MRC process.

The reconstructed process involved almost two hundred of million cubic meters in volume, accommodated by a low angle, up to 250 m deep shear zone. Such ongoing deformation is featured by diagnostic foot-slope bulging and backscarps and deep trenches that are often filled by detritic materials.

MATERIALS AND METHODS

In recent decades, engineering-geological modelling and surface geophysical investigations have been largely used for SM and local seismic response studies (Delgado *et alii*, 2000; Lebrun *et alii*, 2006; Icms Working Group, 2008; Lenti *et alii,* 2009; Bozzano *et alii,* 2017) as well as to investigate landslide processes (Bogoslovsky & Ogilvy, 1977; Mccann & Forster, 1990; Hack, 2000; Maurer *et alii*, 2010; Jaboyedoff *et alii,* 2019) as their joint application is useful to define fundamental features of subsoils or unstable masses and to assess and validate the expected behaviour in the case of seismic shaking.

In this study, an engineering-geological modelling was carried out to reconstruct the geological setting of the Forio municipal

area and to define the physical and mechanical properties of the outcropping soils and rocks; at the same time, several single-station seismic ambient noise measurements were performed to validate and integrate the reconstructed subsoil model as well as to evaluate how some peculiar complexities of the Ischia island geology could affect the local seismic response.

Engineering-geological modelling

A detailed engineering geological model has to lay on high resolution geological surveys and subsoil investigations aimed to define its fundamental geological features and main relationships between surface bodies or covers and the bedrock. In this case, previously performed surveys and borehole investigations allowed us to delineate a more detailed geological model of the study area and to analyse the influence of the geological features on the local seismic response.

The reconstructed engineering geological model, summarised in the enclosed Table with map and cross section of interest, represents a synthetic view based on the geological maps and geotechnical and geothermal surveys available in literature. Lithostratigraphic and volcanological units identified in literature were grouped and transposed into Synthetic Units in virtue of their main litotechnical properties as listed in Annex 2 and reported in Map.

During the survey campaign performed in November 2017 after the 21st August event, the Campania Region provided the consultation of a database of wells and boreholes related to the surveys carried out in the Ischia island in the last decades. The latter includes 55 boreholes in the territory of Forio; moreover, 5 further stratigraphic logs were derived from technical studies.

About 20% of these investigations are localised in Forio city centre since they were used for the engineering design and geothermal exploration for thermal resorts and spas. Other surveys were carried out in the northern part of the Municipality of Forio, close to the Zaro promontory and in the Mt. Nuovo sector. The average depth of the boreholes is 87 m and often they exceed the usual depth of 30-m required by technical regulation for V_s30 quantification.

The borehole data report a description of the lithologies encountered during drilling obtaining information on the thickness of the different geological layers. It is worth noting that 25% of boreholes reach the compact MEGT, which can be considered as geological bedrock due to its reduced alteration and high welding and stiffness. The consultation of the survey database made it possible to summarize the observations in the diagrams of Fig. 3.

The consultation of the boreholes data made it possible to summarise the observations reported in Fig. 3. In fact, Fig. 3a shows the frequency distribution of lithological classes drilled in the boreholes while the histogram of Figure 3b shows the percentage of thickness for each lithological class in different range of depth, allowing to correctly interpret the frequency of each lithological class with depth resulting by the database. As it results from the diagram, landslide deposits ascribable to debris avalanches (Da), debris flow (Df) and shallow landslides (Ld) were mainly drilled up to 50 m b.g.l. while the deepest boreholes cored pyroclastic deposits (PSlo) as well as massive and lithoid tuffs (GT) and lavas (La).

Other site geophysical investigations carried out in the Municipality of Forio include Multi-channel Analysis of Surface

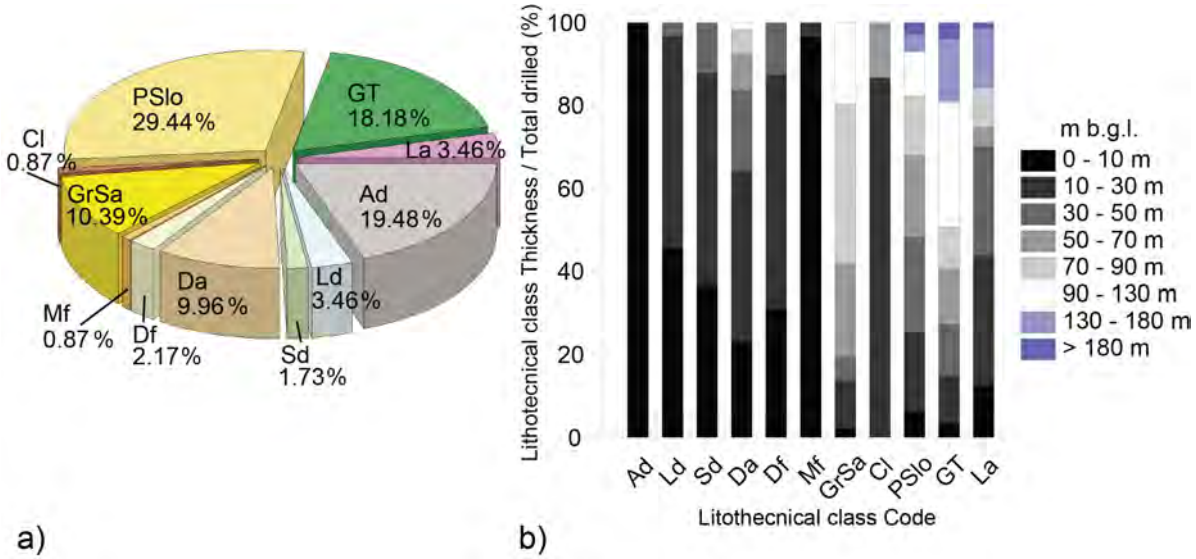

Fig. 3 - a) Distribution of the lithology classes as it results from from the analysis of borehole log-stratigraphies; b) distribution of the class thickness percentage, in depth range, as it results from the analysis of borehole log-stratigraphies. In Fig. 2 the lithological class codes are explained

Waves (MASW) surveys performed by professionals in the period from 2008 to 2017 and devoted to the characterisation of the studied areas in terms of shear-wave velocity (Vs) profiles (see enclosed map for location). They are mainly located in the coastal plain of Forio within the urban centre. The MASW results points out a Vs velocity profile with values below 300 m/s down to about 15 m depth, characteristic values of soft soils and shallow covers.

The engineering-geological map of the Municipality of Forio as derived from the borehole data as well as from direct geological surveying is reported in Plate 1. Annex 2 reports the assumed transposition between geological and lithotechnical units as they were reported in the engineering-geological map of Plate 1 and Fig. 3.

Single-station seismic ambient noise measurements

Seismic ambient noise was recorded in 142 single-station measurement points distributed over the whole Forio municipal area during several field campaigns carried out between 2014 and 2017 (see Plate 1). Three different seismic data acquisition equipments were used: i) SL06 24-bit dataloggers set to a sampling frequency of 200 Hz with a built-in SS20 three-component velocimetric sensor (2 Hz eigenfrequency) produced by SARA Electronic Instruments; ii) LE-3D/5s 3-component seismometers by Lennartz Electronic GmbH coupled with RefTek 130-01 dataloggers set to a sampling frequency of 250 Hz; iii) Tromino® 3-component portable tromometers with 128 Hz sampling frequency. Each measurement lasted between 30 and 75 minutes, even if most of them had a duration of 1 hour. Seismic ambient noise measurements were analysed by using two different approaches: i) the standard Horizontal-to-Vertical Spectral Ratio (HVSR) analysis; ii) the Time-Frequency Polarization Analysis (TFPA).

The HVSR analysis, proposed by Nogoshi & Igarashi (1970, 1971) and analytically implemented by Nakamura (1989), is a reliable tool to evaluate the resonance frequency of a site (f_0). The HVSR functions represent the ratio between horizontal and vertical Fourier spectra at each natural frequency and, according to Bonnefoy-Claudet *et alii* (2006), a peak in these functions can be related to a SH-wave resonance in soft surface layers or can be due to the ellipticity of particle motion when the ambient noise is composed mainly of fundamental mode Rayleigh waves.

The HVSR analysis is traditionally applied in SM or local seismic studies to evaluate the presence of resonance of low shear-wave velocity layers (i.e., soft soil) above a stiff rock (i.e., seismic bedrock), especially if a marked impedance contrast exists (Bour *et alii*, 1998; Haghshenas *et alii*, 2008). In fact, a clear peak in the HVSR function can be observed when a sedimentary sequence acts as a resonant layer above a seismic bedrock composed of stiff rocks (SESAME, 2004); the HVSR peak can be easily associated to a 1D stratigraphic resonance if it does not present directional features, i.e., absence of polarization, and the associated 3-component Fourier amplitude spectra have the typical "eye-shape" (Castellaro & Mulargia, 2009), i.e., an increase of the horizontal spectral components and a decrease of the vertical spectral component around the peak frequency.

Recently, the HVSR analysis was used also in non-conventional conditions to evaluate any possible changes occurring in the seismic wavefield in the case of particular geological settings, such as rock masses characterised by different jointing conditions (Panzera *et alii*, 2012; Galea *et alii,* 2014; Valentin *et alii,* 2017; Iannucci *et alii,* 2018, 2020; D'Amico *et alii,* 2019; Martino *et alii*, 2020).

In this work, the HVSR functions were obtained by Geopsy software (Wathelet *et alii*, 2020): the Fast Fourier Transform (FFT) was computed for the three ground-motion components (North-South, East-West and Up-Down) on 40-s non-overlapping time windows with 5% cosine taper and the obtained FFT spectra were smoothed by the Konno & Ohmachi (1998) function; then, the HVSR for each time window was computed as ratio between the quadratic mean of the horizontal components (H) and the vertical component (V); finally, single-window HVSR were averaged to obtain the HVSR function. In addition, the specific tool of Geopsy was used to analyse the HVSR variation as a function of the considered horizontal direction for observing any possible directivity: the average HVSR was computed rotating the horizontal components from 0° to 180° every 10° and was plotted in a frequency-azimuth plot.

The seismic ambient noise records were also processed by the TFPA method using the WAVEPOL code (Burjánek *et alii*, 2012), that implements the analysis of ellipticity and polarization of the particle motion introduced by Vidale (1986). The WAVEPOL code uses the Continuous Wavelet Transform (CWT) for representing the particle motion at each time-frequency pair as a 3D ellipse; the ellipticity is expressed as the ratio between the semi-minor axis and the semi-major axis of the ellipse (i.e., 1 for circular motion and 0 for linear motion) while the polarization is indicated in terms of strike, i.e., the azimuth of the semi-major axis projected to the horizontal plane with respect to North, and dip, i.e., the dip angle of the semi-major axis with respect to the horizontal plane.

TFPA method was used for the identification of frequency-dependent directional resonances in jointed rock masses characterised by anisotropies (Burjánek *et alii*, 2010, 2012, 2014; D'Amico *et alii*, 2019; Panzera *et alii*, 2019) or unstable rock blocks (Galea *et alii*, 2014; Iannucci *et alii*, 2018, 2020; D'Amico *et alii*, 2019), evidencing a polarization of the particle motion roughly perpendicular to the anisotropy/fracture directions associated with a high degree of linearity in the case of oscillating blocks.

RESULTS

The results obtained by the analysis of seismic ambient noise measurements performed in the Municipality of Forio are here presented, with particular emphasis regarding the three selected areas characterised by the above-described geological complexities: i) the Zaro promontory; ii) the lahar of Forio and iii) the Mt. Nuovo deforming slope.

All the seismic ambient noise measurements (Annex 1) were analysed according to the HVSR (Nakamura, 1989) method, while the TFPA was used only for the measurements carried out in the three selected areas.

For each measurement, the analysis results were summarised by evidencing some specific peculiarities: for the HVSR analysis, the frequency value corresponding to the main peak with the highest amplitude (f_0) and, if present, the frequency value corresponding to the secondary peak with a lower amplitude level (f_1); for the TFPA, the frequency values (f_I, f_{II}) characterised by linearity (i.e., ellipticity lower than 0.2) and/or polarization of the particle motion having a significant frequency of occurrence (i.e., at least 50%). In the case of absence of HVSR peak, the measurement was classified as not resonant (NR).

Most of the 142 seismic noise measurements show HVSR curves with a main resonance at very low frequency, about 0.4-0.5 Hz, often with a peak uncertain in shape or amplitude. These resonance values are challenging to be related to other available geological and geophysical data (such as MASW and borehole data) as they are related to an impedance contrast that is supposed to be several hundred meters deep, perhaps corresponding to the roof of the ancient fractured trachytic lavas. Only in the Baia di Citara area, the resonance rises to values of 0.6 Hz.

Additional HVSR peaks in a range of frequencies between 2 and 11 Hz, often with amplitude higher than the ones at 0.4-0.5 Hz, were pointed out in 44 seismic noise measurements, mainly grouped in the three analysed sectors.

Zaro promontory

Local seismic response of the lava Zaro promontory was investigated through 13 seismic ambient noise measurements (Table 1) and other 10 in the surroundings lined up along with and across the main fractures that dissect the area of Zaro (Fig. 2a).

The results point out a main HVSR resonance peak in a range between 7 Hz and 9 Hz and a secondary HVSR peak at 0.4 Hz at stations FO30S, FO163S, FO171S, FO173S and FO174S (Fig. 4, left and middle panels), aligned following the trace of the NW-SE fracture set at the eastern side of the promontory. The secondary HVSR peak presents also FFT spectra characterised by the "eye-shape" trend. For the same measurements, the TFPA results evidence a regular ellipticity (i.e., no linearity) and slight features of polarization of the particle motion for the frequency values corresponding to the main HVSR peak, while neither anomalies in the ellipticity nor polarization were observed at 0.4 Hz. According to the obtained results, the secondary HVSR peak can be assumed as relative to a 1D resonance, characteristic of the entire study area, caused by the presence of the deep bedrock, while the main HVSR peak could be due to the outcropping lava and could be influenced by the disjointing element.

On the other hand, the measurements FO30S, FO170S and FO172S (Fig. 4, right panel) only show a resonance at 3-4 Hz without the presence of other HVSR peaks at the lower frequencies (Fig. 4), except for the FO30S that has the secondary peak at 0.4 Hz related to the 1D resonance. The TFPA evidence quite marked features of linearity and polarization of the particle motion at 3-4 Hz (Fig. 4, right panel).

Lahar of Forio

A total of 27 seismic ambient noise measurements were carried out in the Forio city centre and the nearby the peripheral areas (Tab. 2). The geological peculiarity of this sector is the presence of a surficial lahar deposit extended from the foot of

Code	HVSR analysis			TFPA									
	f_0 (Hz)	f_0 HVSR amplitude	f_1 (Hz)	f_I (Hz)	f_I ellipticity	f_I ellipticity occurrence (%)	f_I polarization (°)	f_I polarization occurrence (%)	f_{II} (Hz)	f_{II} ellipticity	f_{II} ellipticity occurrence (%)	f_{II} polarization (°)	f_{II} polarization occurrence (%)
FO30S	4	6	0.4	2	0.3	80	45	50	4	0.15	80	45	30
FO38S	0.4	3	-	2	0.3	80	20	50	4	0.2	90	20	30
FO105S	NR	-	-	1.5	0.35	50	70	30	-	-	-	-	-
FO154T	7.7	3	4.5	-	-	-	-	-	-	-	-	-	-
FO155S	0.4	2	-	0.6	0.3	70	10	60	1.5	0.35	60	10	70
FO163S	8	4	0.3	1.5	0.3	60	10	50	8	0.2	80	10	40
FO164R	-	-	-	4	0.15	90	0	50	-	-	-	-	-
FO169S	-	-	-	3	0.2	80	20	80					
FO170S	3.5	3	-	1.5	0.25	60	0	70	4.5	0.25	80	165	50
FO171S	9	3.5	0.4	2	0.4	60	50	50	9	0.2	80	60	50
FO172S	3	3.5	-	3	0.1	90	150	90	-	-	-	-	-
FO173S	6.7	4	-	6	0.15	90	65	70	-	-	-	-	-
FO174S	9	3	0.4	2	0.3	70	40	30	-	-	-	-	-

Tab. 1 - Results obtained by the HVSR analysis and TFPA for the seismic ambient noise measurements performed at the Zaro promontory

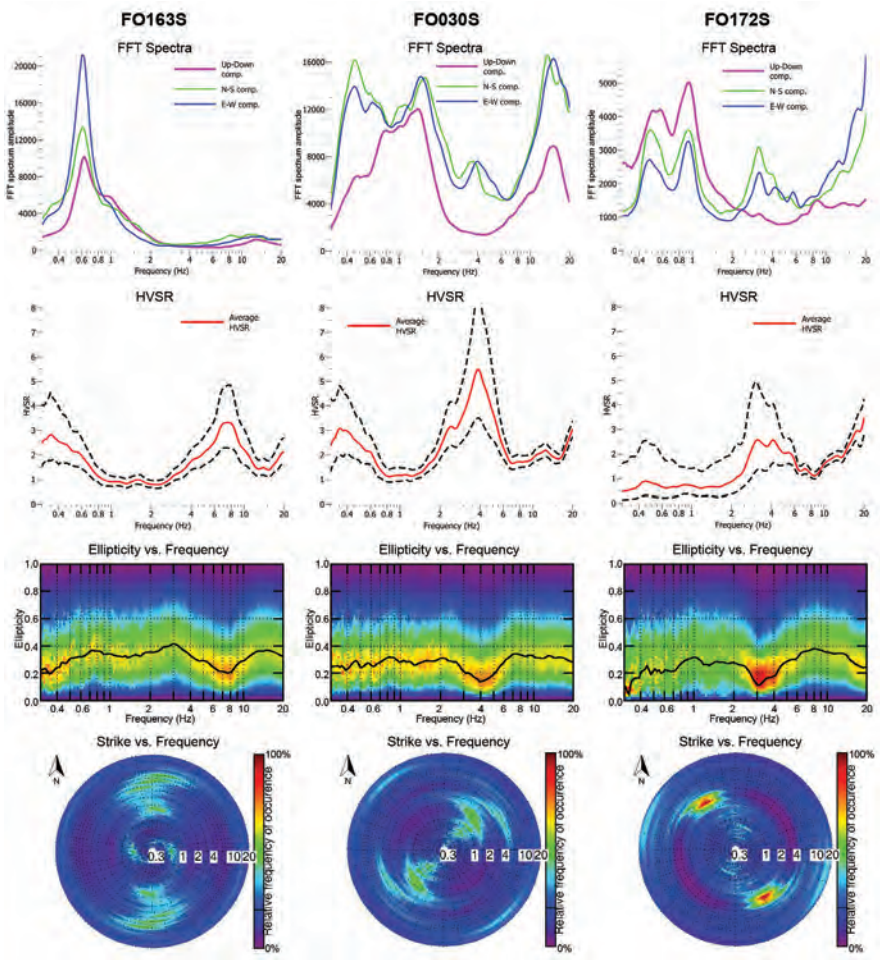

Fig. 4 - Examples of FFT spectra, HVSR function (the dashed black lines show the standard deviation of the curve), ellipticity diagram and polar strike plot (same palette colour for relative frequency of occurrence) obtained at the Zaro promontory. See Plate 1 for the location of the measurement stations

Mt. Nuovo slope toward the seashore (Fig. 2b).

The single-station seismic ambient noise measurements were conducted following two main alignments, one transverse and one longitudinal to the body of the lahar, in order to try to reconstruct its thickness in different zones (i.e., distal, apical, and lateral with respect to its maximum extension).

As a general remark, the results (Fig. 5) point out an average HVSR resonance peak at 0.4-0.7 Hz for all measurement stations at the Forio lahar. This HVSR peak presents an "eye-shape" of the FFT spectra and a regular value of ellipticity without evidence of polarization of the particle motion according to the TFPA results. For these reasons, the HVSR peak at 0.4-0.7 Hz can be associated with a 1D resonance, which can be related to the seismic impedance contrast between a lava main bedrock and the MEGT deposits considering the local geological setting of the volcanic deposits (Moscatelli *et al.*, 2020). Only in the measurements, carried out inside the body of the lahar, a secondary f_1 HVSR peak can be observed in a range between 4 Hz and 12 Hz. Since the f_1 HVSR peak presents FFT spectra with "eye-shape", regular ellipticity and no polarization, it can be related to the presence of the lahar deposits overlaid to MEGT that produce a 1D resonance. At the same time, its different frequency value can be attributable to the variable thickness of the lahar.

Taking into account the cross-section WNW-ESE oriented (i.e., along the major axis of the lahar, Figure 8), the f_1 values change from about 12 Hz to about 4 Hz moving from the apical area of the lahar deposit to the distal one, thus showing a thickening of the deposit in the same direction. In the longitudinal section NNE-SSW oriented (i.e., along the minor axis of the lahar), the f_1 value appears to be lower in the centre of the lahar deposit than at his border (i.e., so testifying a higher thickness in the central areas), disappearing outside this boundary.

Code	HVSR analysis			TFPA										
	f_0 (Hz)	f_0 HVSR amplitude	f_1 (Hz)	f_I (Hz)	f_I ellipticity	f_I ellipticity occurrence (%)	f_I polarization (°)	f_I polarization occurrence (%)	f_{II} (Hz)	f_{II} ellipticity	f_{II} ellipticity occurrence (%)	f_{II} polarization (°)	f_{II} polarization occurrence (%)
FO01S	-	-	-	-	-	-	-	-	-	-	-	-	-
FO02R	0.5	5	-	0.5	0.15	80	30	30	-	-	-	-	-
FO03S	0.5	3	6	0.5	0.25	80	40	30	6	0.3	60	40	30
FO04S	NR	-	-	-	-	-	-	-	-	-	-	-	-
FO05R	NR	-	-	-	-	-	-	-	-	-	-	-	-
FO06R	0.5	5.5	4	0.5	0.15	80	40	20	4	0.3	50	20	30
FO07S	0.7	4	6.5	0.5	0.2	80	70	30	6	0.3	70	40	30
FO08S	0.5	5	3	0.5	0.2	90	20	30	-	-	-	-	-
FO09R	0.5	4	-	0.5	0.2	90	160	40	-	-	-	-	-
FO10R	0.5	6	10	0.5	0.2	80	40	30	10	0.3	70	100	30
FO11R	0.7	5	8	0.7	0.2	80	40	20	-	-	-	-	-
FO13R	NR	-	-	0.8	0.2	80	110	30	3	0.35	50	150	50
FO14R	0.4	3	-	0.4	0.2	80	170	50	-	-	-	-	-
FO16S	0.8	3.5	-	0.8	0.2	80	180	30	4	0.35	60	135	30
FO18T	0.4	3.5	10	0.4	0.1	90	170	50	4	0.4	60	170	40
FO26S	0.7	3	8	0.5	0.2	90	170	50	-	-	-	-	-
FO27S	0.8	4	-	0.8	0.15	90	180	30	-	-	-	-	-
FO31S	0.5	4	8	0.4	0.15	80	50	40	-	-	-	-	-
FO32S	0.5	3.5	-	0.5	0.2	80	40	40	-	-	-	-	-
FO33S	0.5	5	-	0.5	0.15	90	60	30	10	0.3	50	110	40
FO37S	0.5	4	-	0.4	0.2	90	30	30	-	-	-	-	-
FO103S	0.4	5	-	0.4	0.15	90	30	30	3	0.35	60	90	40
FO106S	0.4	5	-	0.4	0.2	90	20	30	-	-	-	-	-
FO141S	0.5	4	-	0.6	0.2	90	20	30	-	-	-	-	-
FO147S	0.5	5.5	12	0.5	0.15	90	80	30	12	0.3	70	20	30
FO151S	0.5	5	4	0.5	0.2	90	170	40	4	0.3	60	90	40
FO153S	0.5	5	5.5	0.5	0.15	90	40	30	6	0.3	60	30	30

Tab. 2 - Summary of the results obtained by the HVSR analysis and TFPA for the seismic ambient noise measurements performed in the Forio lahars zone

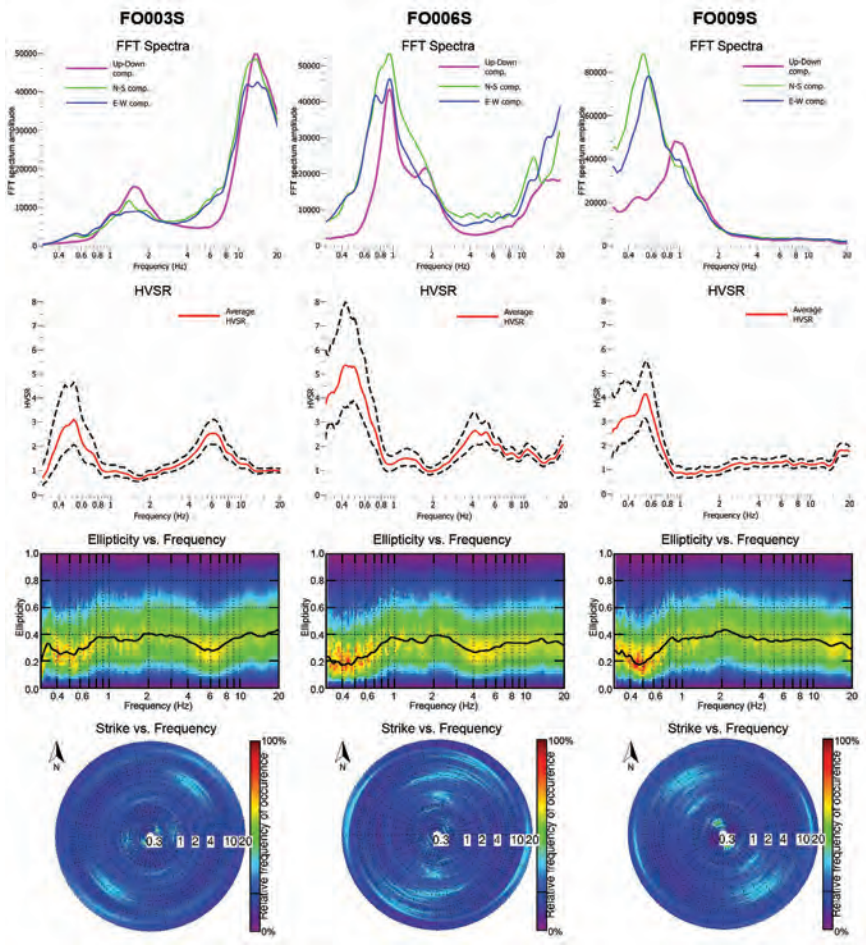

Fig. 5 - Examples of FFT spectra, HVSR function (the dashed black lines show the standard deviation of the curve), ellipticity diagram and polar strike plot (same palette color for relative frequency of occurrence) obtained in the Forio lahar zone. See Plate 1 for the location of the measurement stations

Mt. Nuovo deforming slope

Seismic ambient noise was recorded at the Mt. Nuovo deforming slope through 20 single-station measurements over an area of approximately 1 km^2 (Table 3), along a section that crosses the main surveyed structural and geomorphological features from Mt. Epomeo to Mt. Nuovo (Fig. 2c).

As already described in Della Seta *et alii* (2015), on the Mt. Nuovo deforming slope area the evidence of a 1D resonance frequency was used to indirectly assess the depth of the deformed rock mass (DSGSD of Mt. Nuovo), relating the f_0 value to the thickness of a soft-rock layer that corresponds to the detached rock-mass volume. The thickness estimation was made possible by assuming a Vs value of 800-900 m/s for MEGT, according to the results presented by Strollo *et alii* (2015).

The results (Fig. 6) point out a HVSR resonance peak at about 0.8 Hz at stations ST_1 (Fig 6, left panel), ST_3 and ST_8 (Fig. 6, middle panel), that does not show directivity in terms of linearity and polarization of the particle motion according to the TFPA results. Considering the "eye-shape" characterising the FFT spectra, this resonance could be related to an impedance contrast between a soft-rock layer and a bedrock, under 1D condition. Taking into account the geological features of Mt. Nuovo slope area, the observed HVSR peak at 0.8 Hz could be linked to the presence of a soft layer approximately 250 m thick, constituted within the MEGT, which is part of the landslide mass and overlay the landslide bedrock (Fig. 9). This resonance is no more evident moving from Mt. Nuovo toward the Falanga plain where the MEGT is not yet involved in the landslide process so justifying a more reduced seismic impedance contrasts.

The results from ST_4 measurement, located between the Falanga plain and the top of Mt. Epomeo, are singular since they show a consistent HVSR peak at 7 Hz; in addition, this peak presents "eye-shape" FFT spectra, regular ellipticity and no evidence of polarization (Fig. 6, right panel), therefore it can be associated to a 1D resonance probably due to the presence of a shallow unconsolidated soil, partially made of a rock slide mass and partially of eluvial-colluvial deposits generated by weathering and hydrothermal alteration. Based on the 7 Hz resonance peak and taking into account the Vs values typical for such a kind of deposits (500-600 m/s) it is possible to estimate a thickness of about 15 meters of the debris cover, that is in agreement with the collected evidences (Della Seta *et alii*, 2012, 2015).

The other seismic ambient noise measurements carried out on Mt. Nuovo slope areas do not show significant HVSR peaks; this absence of resonance can be ascribed to the presence of main faults or shear zones that increase the rock mass jointing conditions of both the landslide mass and bedrock, so locally reducing the seismic impedance contrast.

As a general remark on the HVSR results obtained by the geophysical investigations carried out in this sector, several noise measurements show HVSR amplitude higher than 2 within a wide frequency range as the FFT of the horizontal components are generally higher than the vertical ones (Della Seta *et alii*, 2015). This effect could be attributed to a topographic amplification due to peculiar landform geometries like steep slopes or sharp ridges, that control the directional distribution of FFT (Del Gaudio *et alii,* 2007).

Anyway, the TFPA does not evidence features of linearity nor polarization of the particle motion for the seismic ambient noise measurements carried out at Mt. Nuovo, confirming the absence of these effects in the case of DSGSD-involved slopes as already observed in Central Apennines by Martino *et alii* (2020).

Code	HVSR analysis			TFPA									
	f_0 (Hz)	f_0 HVSR amplitude	f_1 (Hz)	f_I (Hz)	f_I ellipticity	f_I ellipticity occurrence (%)	f_I polarization (°)	f_I polarization occurrence (%)	f_{II} (Hz)	f_{II} ellipticity	f_{II} ellipticity occurrence (%)	f_{II} polarization (°)	f_{II} polarization occurrence (%)
ST_1	0.8	4.5	2.5	1.5	0.25	80	120	30	-	-	-	-	-
ST_2	NR	-	-	2.5	0.2	80	60	50	6	0.3	75	70	30
ST_3	0.7	3.5	-	20	0.35	60	115	50	-	-	-	-	-
ST_4	7	3.5	0.5	-	-	-	-	-	-	-	-	-	-
ST_5	0.5	3	-	7	0.3	70	175	50	-	-	-	-	-
ST_5b	0.5	3	-	7	0.3	70	165	50	-	-	-	-	-
ST_6	0.4	3.5	-	-	-	-	-	-	-	-	-	-	-
ST_7	0.4	5	-	-	-	-	-	-	-	-	-	-	-
ST_8	0.9	4.5	2.5	-	-	-	-	-	-	-	-	-	-
ST_9	-	-	-	2.5	0.25	80	130	50	-	-	-	-	-
ST_9b	2.5	3.5	4	2.5	0.25	80	120	30	-	-	-	-	-
ST_10	NR	-	-	2	0.25	80	140	30	-	-	-	-	-
ST_10b	-	-	-	2	0.3	80	140	30	-	-	-	-	-
ST_11	-	-	-	20	0.2	80	165	50	-	-	-	-	-
ST_12	0.8	3	4	2	0.3	80	125	50	-	-	-	-	-
ST_13	0.8	3	-	2	0.3	70	120	30	4	0.25	80	140	30
ST_14	NR	-	-	2.5	0.25	80	120	30	5.5	0.3	80	125	30
ST_15	-	-	-	2	0.25	80	120	30	6	0.3	70	150	30
ST_16	0.8	3	-	2.5	0.3	70	120	30	-	-	-	-	-
ST_17	NR	-	-	2.5	0.25	80	120	50	8	0.25	70	110	30

Tab. 3 - Summary of the results obtained by the HVSR analysis and TFPA for the seismic ambient noise measurements performed in the Mt. Nuovo deforming slope area

DISCUSSION

The three case studies selected at Forio (Ischia island) allow us to discuss some specific topics dealing with the role of peculiar

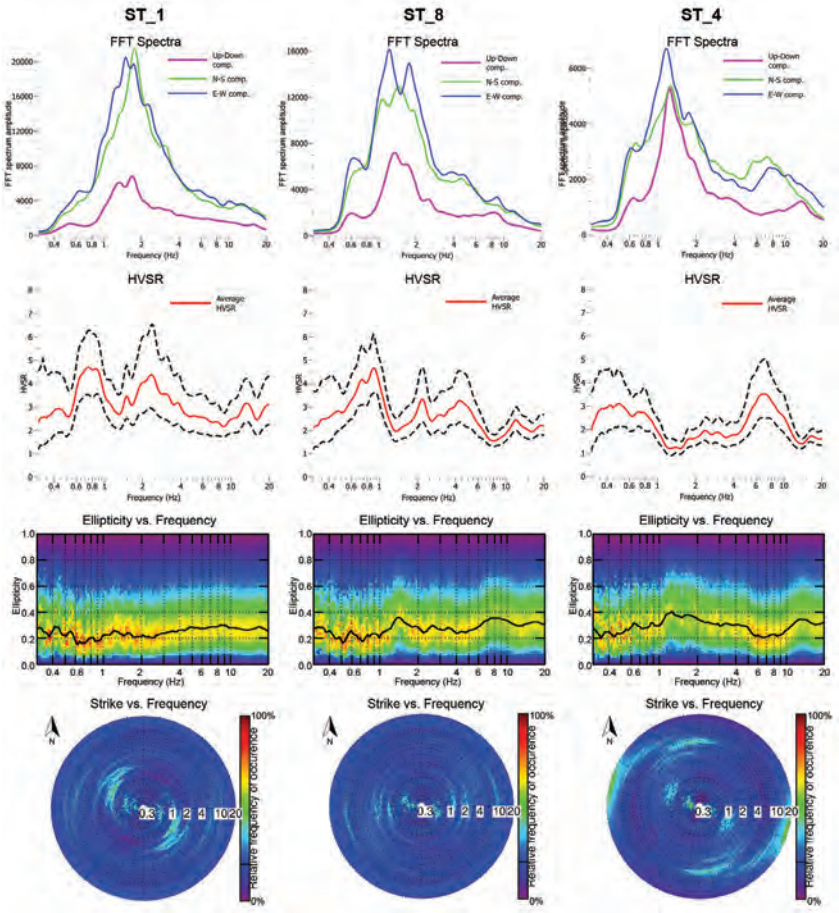

Fig. 6 - Examples of FFT spectra, HVSR function (the dashed black lines show the standard deviation of the curve), ellipticity diagram and polar strike plot (same palette color for relative frequency of occurrence) obtained in the Mt. Nuovo deforming slope area. See Plate 1 for the location of the measurement stations

geological features in local seismic amplification effects. As it regards the Zaro promontory, the evidence of amplification and polarization of the ground motion can be related to Rayleigh waves propagation and linked to their interaction with either jointed zones close to fractures or fault lines (D'Amico *et alii*, 2018) which are surveyed in the promontory inferring more intense jointing conditions in the rock masses (Martino *et alii*, 2006). These results confirm possible amplification effects in outcropping bedrock areas related to anisotropic and/or heterogeneous media; these effects are not negligible even though their areal distribution is limited to the area very close to the structural elements which are retained responsible for the local seismic effects (Fig. 7). In this case, the jointing conditions induce more evident effects also with respect to topographic elements as cliffs or ridges. Moreover, as it is reported in Hailemikael *et alii* (2016), polarization can be observed also in case of stratigraphic amplification (i.e., related to shallow debris covers) if topographic conditions and rock mass anisotropy influence the surface wave propagation. According to this consideration, the presence of 3-4 Hz resonance values in the southern sector of Zaro promontory, could be justified by the presence of a 5 m thick soft-soil with very low Vs, above the trachitic lavas and made up of eluvial-colluvial deposits generated by weathering.

As it regards the Forio plain, where the lahar loose deposit outcrops, the stratigraphic effects on the local seismic response are related to the peculiar geometry of such a geological body, i.e. to its lateral and longitudinal variation of its thickness. As it results from the HVSR outputs in Figure 8, a characteristic HVSR peak at frequency values higher than 3 Hz is visible in the measurement sites within the lahar body. The peak frequency values decrease down to 4 Hz moving forward from the source area (in which the peak frequency shows values up to 10 Hz) as the debris thickness increases, while peak frequency values increase up to 10-12 Hz moving laterally from the middle internal portion of the debris mass toward its external zone, reflecting the thickening and thinning respectively along with or cross to the

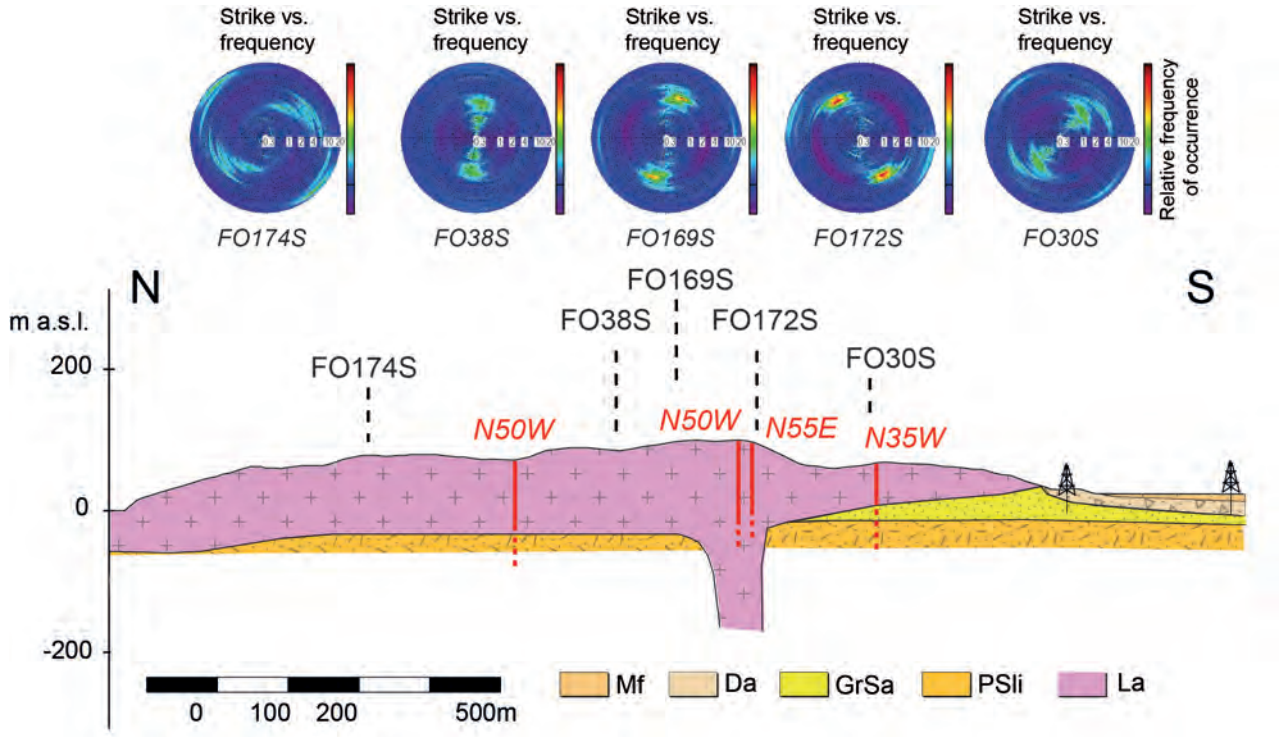

Fig. 7 - Spatial distribution of the TFPA polar strike plots obtained in the Zaro promontory and related results which highlight the polarized amplification related to the main fault and fractures which cause the rock mass jointing

direction of propagation. This HVSR peak is not found, however, immediately outside the lahar borders, thus demonstrating its strict dependence on the presence or absence of the lahar body.

As it regards the deforming slope of Mt. Nuovo, as an effect of the MRC process, evidence of seismic amplification at low frequency values (0.7-1.0 Hz) exists within the involved rock mass even if no polarization is observed (Fig. 9). On the contrary, no resonance effects were observed in the sector of the Falanga plain, where no deforming processes are surveyed. As already discussed in Martino *et alii* (2020) for the slope deforming masses of Tino and Grisciano hamlets (Accumoli, Central Italy), such a response testifies the complexity of resonance effects related to the intensely jointed rock mass within a MRC-controlled deforming volume where the absence of well-defined and oriented structural elements cannot impress a significant anisotropy to the rock mass system and seems not to induce marked effects of polarization and linearity of the particle motion. In addition, since no sliding surface delimits the deforming mass in case of MRC process, a purely stratigraphic effect cannot be invoked to justify the observed seismic response but rather a modified vibrational behaviour of the deforming mass with respect to the undeformed substratum.

The above reported results represent interesting insights in view of SM studies, as it seems possible to account for no conventional interpretation for observed site effects, allowing to introduce further criteria for mapping. Such proposals may include mapping buffer for zoning intense jointed rock masses astride fault lines or fracture alignment where ground-motion amplification and polarization are observed. Moreover, a seismic amplification can be also attributed to unstable zones, as in case of landslide slopes, in order to consider a combined effect posed by geomorphological and seismic hazards. The considered case histories demonstrate the significant role of passive seismic geophysics for zoning geological bodies as well as ongoing deformations on slopes; even if not conventional interpretation could be provided in terms of purely stratigraphic seismic response, evidence of amplification can be related to zones characterized by specific geological elements especially in view of seismic microzonation studies.

In view of engineering-geological modelling, few-time consuming noise measurements proved their suitability for detecting those geological features and/or structural elements which interact with seismic wave propagation by a combined HVSR and TFPA processing. Moreover, following the present guidelines for SM studies in Italy, a level 1 could account approximately for the aforementioned features while a level 3 could define sub-zones attributing them quantitative properties in terms of amplification factors and subsoil dynamic properties.

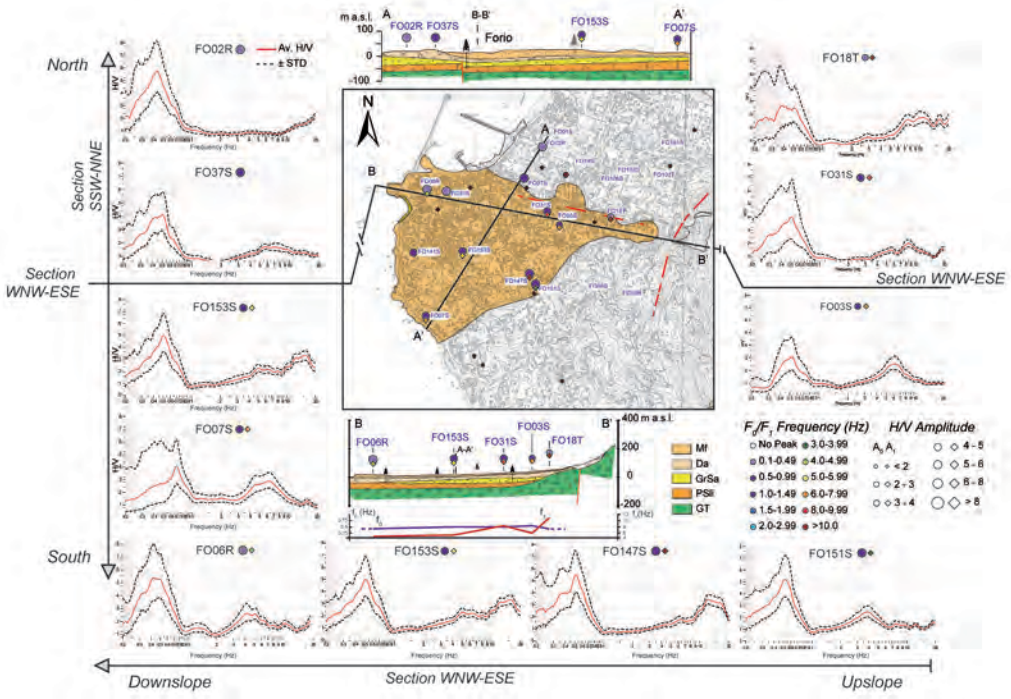

Fig. 8 - Spatial distribution of the HVSR functions obtained in the Forio plain and related results which highlight the 1D stratigraphic resonance related to the peculiar geometry of the lahar deposits. See Plate 1 for the location of the measurement stations

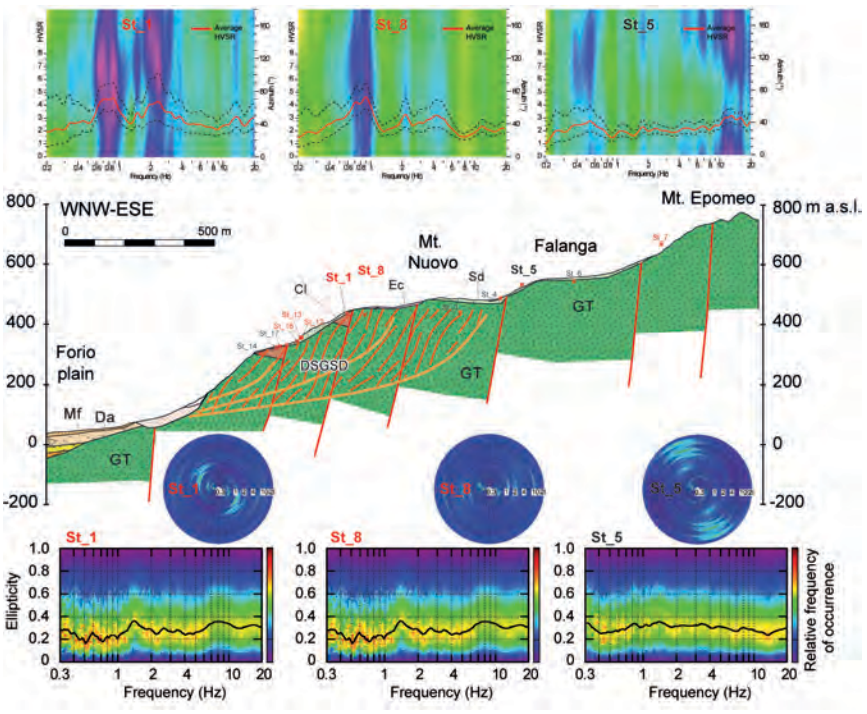

Fig. 9 - Distribution along a geological cross section of the results obtained from the ambient noise measurements performed in the Mt. Nuovo deforming area highlighting the resonance related to the mass involved in the MRC process. See Plate 1 for the location of the measurement stations

CONCLUSIONS

The study of local seismic response performed in the Municipality of Forio in Ischia has made possible to highlight some peculiarities strictly connected to geological complexities, which result from a rather recent volcano-tectonic and depositional evolution, as it can be traced back to the last tens of thousands of years.

In particular, evidence of polarized amplification can be related to the presence of discontinuities inherited from faults and fracture sets in the sector of the Zaro promontory. Evidence of stratigraphic amplification connected to the overlaying of volcanic depositional bodies on deposits of debris and rock avalanches which characterize the sector of Forio city centre and highlight the lateral variations of the aforementioned deposits, limited to a few hundred meters, in relation to the remarkable variations of the peaks in the HVSR functions. Lastly, the ongoing gravity-induced MRC deformations in the sector of the Mt. Nuovo slope justify more intense jointing conditions for the rock mass involved, delimiting a resonant volume which is elicited from the surrounding substrate.

The three selected cases report conceptual models of response respectively 1D (for Forio lahar), 2D (for Zaro promontory) and 3D (for Mt. Nuovo deforming slope) thus demonstrating the relevance of the engineering-geological modelling of rock mass and/or deposit volumes and its fundamental role, especially in very geologically complex contexts.

The results of the analysis here presented also highlight the need to extend the categories of homogeneous seismic response zones, especially in the products of MS1 (MOPS maps) to take into account, in a distinct form, the possible amplification effects in jointed rock mass involved in gravity-induced deformation processes. The current guidelines, in fact, do not codify the slope deformation processes for MRC as unstable areas due to landslides (i.e., ZA_{FR}), while on the other hand they can be fully or partially amplified.

ACKNOWLEDGEMENTS

The Authors wish to thank the Municipality of Forio di Ischia for allowing the field surveys and geophysical investigations; they also thank the Campania Region Technical Office for allowing the consultation of the database with the boreholes log-stratigraphies. M. Della Seta, M. Fiorucci, G.M. Marmoni and S. Martino, performed geomorphological and engineering-geological surveys; P. Caprari, M. Fiorucci, R. Iannucci, G.M. Marmoni, A. Paciello and G. Martini performed the geophysical investigations and analysis; C. Esposito supervised the engineering-geological data acquisition and analysis; M. Della Seta supervised the geomorphological data acquisition and analysis; S. Hailemichael and S. Martino supervised the geophysical data acquisition and analysis; G.M. Marmoni, G. Martini and A. Peloso performed the data mapping; P. Caprari collected the borehole data and managed the Campania Region database; S. Martino coordinated the scientific activities; all the Authors participated in data interpretation and manuscript writing.

REFERENCES

Azzaro R. , Del Mese S., Martini G., Paolini S., Screpanti A., Verrubbi V. & Tertulliani A. (2017) - *QUEST- Rilievo macrosismico per il terremoto dell'isola di Ischia del 21 agosto 2017,* Rapporto interno, Doi:10.5281/zenodo.849091.

Bogoslovsky V.A. & Ogilvy A.A. (1977) - *Geophysical methods for the investigation of landslides*. Geophysics, **42** (3): 562-571.

Bonnefoy-Claudet S., Cotton F. & Bard P.-Y. (2006) - *The nature of noise wavefield and its applications for site effects studies: a literature review.* Earth-Sci. Rev., **79** (3): 205-227.

Bour M., Fouissac D., Dominique P. & Martin C. (1998) - *On the use of microtremor recordings in seismic microzonation*. Soil Dyn. Earthq. Eng., **17** (7-8): 465-474.

Bozzano F., Buccellato A., Coletti F., Martino S., Marra F., Rivellino S. & Varone C. (2017) - *Analysis of the seismic site effects along the ancient Via Laurentina (Rome).* Ann. Geophys., **60** (4): 0435.

Brown R.J., Orsi G. & De Vita S. (2008) - *New insights into late Pleistocene explosive volcanic activity and caldera formation on Ischia (southern Italy).* Bull. Volcanol., **70**: 583-603.

Burjánek J., Edwards B. & Fäh D. (2014) - *Empirical evidence of local seismic effects at sites with pronounced topography: a systematic approach.* Geophys. J. Int., **197** (1): 608-619.

Burjánek J., Gassner-Stamm G., Poggi V., Moore J.R. & Fäh D. (2010) - *Ambient vibration analysis of an unstable mountain slope*. Geophys. J. Int., **180** (2): 820-828.

Burjánek J., Moore J.R., Yugsi Molina F.X. & Fäh D. (2012) - *Instrumental evidence of normal mode rock slope vibration*. Geophys. J. Int., **188** (2): 559-569.

Carlino S., Somma R., Troiano A., Di Giuseppe M.G., Troise C. & De Natale G. (2014) - *The geothermal system of Ischia Island (southern Italy): Critical review and sustainability analysis of geothermal resource for electricity generation.* Renew. Energy, **62**: 177-196.

Castellaro S. & Mulargia F. (2009) - *The effect of velocity inversions on H/V.* Pure Appl. Geophys., **166**: 567-592.

D'amico S., Panzera F., Martino s., Iannucci R., Paciello A., Lombardo G., Galea P. & Farrugia D. (2019) - *Ambient noise techniques to study*

near-surface in particular geological conditions: a brief review. In: Persico R., Piro S. & Linford N. (eds) - *Innovation in near-surface geophysics.* 419-460 Elsevier, Amsterdam (NL).

De Vita S., Di Vito M., Gialanella C. & Sansivero F. (2013) - *The impact of the Ischia Porto tephra eruption (Italy) on the Greek colony of Pithekoussai.* Quat. Int., **303:** 142–52.

De Vita S., Sansivero F., Orsi G. & Marotta E. (2006) - *Cyclical slope instability and volcanism related to volcano-tectonism in resurgent calderas: the Ischia island (Italy) case study.* Eng. Geol., **86**: 148–165.

De Vita S., Sansivero F., Orsi G., Marotta E. & Piochi M. (2010) - *Volcanological and structural evolution of the Ischia resurgent caldera (Italy) over the past 10 ky.* Geol. Soc. Am. Spec. Pap., **464**: 193-239.

Del Gaudio V. & Wasowski J. (2007) - *Directivity of slope dynamic response to seismic shaking.* Geophys. Res. Lett., 34, L12301.

Della Seta M., Esposito C., Marmoni G.M., Martino S., Paciello A., Perinelli C. & Sottili G. (2015) - *Geological constraints for a conceptual evolutionary model of the slope deformations affecting Mt. Nuovo at Ischia (Italy).* Ital. J. Eng. Geol. Environ., **2**: 15–29.

Della Seta M., Marotta E., Orsi G., De Vita S., Sansivero F. & Fredi P. (2012) - *Slope instability induced by volcano-tectonics as an additional source of hazard in active volcanic areas: The case of Ischia island (Italy).* Bull. Volcanol., **74**: 79–106.

Delgado J., López Casado C., Giner J., Estévez A., Cuenca A. & Molina S. (2000) - *Microtremors as a geophysical exploration tool: applications and limitations.* Pure Appl. Geophys., **157** (9): 1445-1462.

Galea P., D'amico S. & Farrugia D. (2014) - *Dynamic characteristics of an active coastal spreading area using ambient noise measurements-Anchor Bay, Malta.* Geophys. J. Int., **199**: 1166–1175.

Guidoboni E., Ferrari G., Mariotti D., Comastri A., Tarabusi G., Valensise G. (2007*) - CFTI4Med, Catalogue of strong Earthquakes in Italy (461 B.C.-1997) and Mediterranean Area (760 B.C.-1500),* INGV-SGA, http://storing.ingv.it/cfti4med/.

Hack R. *(2000) - Geophysics for slope stability.* Surv. Geophys., **21**: 423-448.

Haghshenas E., Bard P.-Y., Theodulidis N. & Sesame Wp04 Team (2008) - *Empirical evaluation of microtremor H/V spectral ratio.* Bull. Earthq. Eng., **6**: 75-108.

Hailemikael S., Lenti L., Martino S., Paciello A., Rossi D., & Scarascia Mugnozza G (2016) - *Ground-motion amplification at the Colle di Roio ridge, central Italy: a combined effect of stratigraphy and topography.* Geophys. J. Int., **206** (1): 1-18.

Heap M.J., Kushnir A., Griffiths L., Wadsworth F.B., Marmoni G.M., Fiorucci M., Martino S. & Baud P. (2018) - *Fire resistance of the Mt. Epomeo Green Tuff, a widely-used building stone on Ischia Island (Italy).* Volcanica, **1**(1): 33-48.

Iannucci R., Martino S., Paciello A., D'amico S. & Galea P. (2018) - *Engineering geological zonation of a complex landslide system through seismic ambient noise measurements at the Selmun promontory (Malta).* Geophys. J. Int., **213** (2):1146-1161.

Iannucci R., Martino S., Paciello A., D'amico S. & Galea P. (2020) - *Investigation of cliff instability at Għajn Ħadid Tower (Selmun Promontory, Malta) by integrated passive seismic techniques.* J. Seismol., **24** (4): 897-916.

Icms Working Group (2008) - *Indirizzi e criteri per la microzonazione sismica* – Guidelines for seismic microzonation. Conferenza delle Regioni e delle Province autonome. Dipartimento della Protezione Civile, Roma, 3 vol. e CD-rom. http://www.protezionecivile.gov.it/jcms/it/view_pub.wp?contentId=PUB1137

Jaboyedoff M., Del Gaudio V., Derron M.H., Grandjean G. & Jongmans D. (2019) - *Characterizing and monitoring landslide processes using remote sensing and geophysics.* Eng. Geol., **259**: 105167.

Kleinbrod U., Burjánek J., & Fäh D. (2017) - *On the seismic response of instable rock slopes based on ambient vibration recordings.* Earth Planets Space, **69** (1): 1-9.

Konno K. & Ohmachi T. (1998) - *Ground-motion characteristics estimated from spectral ratio between horizontal and vertical components of microtremor.* Bull. Seism. Soc. Am., **88**: 228-241.

Lebrun B., Duval A.M., Bard P.-Y., Monge O., Bour M., Vidal S. & Fabriol H. (2004) - *Seismic Microzonation: A Comparison between Geotechnical and Seismological Approaches in Pointe-à-Pitre (French West Indies).* Bull. Earthq. Eng., **2**: 27-50.

Lenti L., Martino S., Paciello A. & Scarascia Mugnozza G. (2009) - *Evidence of Two-Dimensional Amplification Effects in an Alluvial Valley (Valnerina, Italy) from Velocimetric Records and Numerical Models.* Bull. Seism. Soc. Am., **99** (3): 1612-1635.

Marmoni G.M., Martino S., Heap M.J. & Reuschlé T. (2017a) - *Gravitational slope-deformation of a resurgent caldera: New insights from the mechanical behaviour of Mt. Nuovo tuffs (Ischia Island, Italy).* J. Volcanol. Geotherm. Res., **345**: 1-20.

Marmoni G.M., Martino S., Heap M. J. & Reuschlé T. (2017b) - *Multiphysics laboratory tests for modelling gravity-driven instabilities at slope scale.* Procedia Engineering, **191**: 142-149.

Martino S., Minutolo A., Paciello A., Rovelli A., Mugnozza G.S. & Verrubbi V. (2006) - *Evidence of amplification effects in fault zone related to rock mass jointing.* Nat. Hazards, **39** (3): 419-449.

Martino S., Cercato M., Della Seta M., Esposito C., Hailemikael S., Iannucci R., Martini G., Paciello A., Scarascia Mugnozza G., Seneca D. &

Troiani F. (2020) - *Relevance of rock slope deformations in local seismic response and microzonation: Insights from the Accumoli case-study (central Apennines, Italy).* Eng. Geol., **266**:105427.

Maurer H., Spillmann T., Heincke B., Hauck C., Loew S., Springman S.M. & Green A.G. (2010) - *Geophysical characterization of slope instabilities.* First Break, **28** (8): 53-61.

Mccann D.M. & Forster A. (1990) - *Reconnaissance geophysical methods in landslide investigations.* Eng. Geol., **29**: 59-78.

Molin P., Acocella V. & Funiciello R. (2003) - *Structural, seismic and hydrothermal features at the border of an active intermittent resurgent block: Ischia Island (Italy).* J. Volcanol. Geotherm. Res., **121**: 65-81.

Moscatelli M., Vignaroli G., Pagliaroli A., Razzano R., Avalle A., Gaudiosi I., Giallini S., Mancini M., Simionato M., Sirianni P., Sottili G., Bellanova J., Calamita G., Perrone A., Piscitelli S. & Lanzo G. (2020) - *Physical stratigraphy and geotechnical properties controlling the local seismic response in explosive volcanic settings: the Stracciacappa maar (central Italy).* Bulletin of Engineering Geology and the Environment. https://Doi.org/10.1007/s10064-020-01925-5.

Nakamura Y. (1989) - *A method for dynamic characteristics estimation of subsurface using microtremor on the ground surface.* Quarterly Report of Railway Technical Research Institute (RTRI), **30** (1): 25-33.

Nogoshi M. & Igarashi T. (1970) - *On the propagation characteristics of microtremors.* J. Seism. Soc. Japan., **23**: 264-280. (in Japanese with English abstract).

Nogoshi M. & Igarashi T. (1971) - *On the amplitude characteristics of microtremors.* J. Seism. Soc. Japan., **24**: 24-40. (in Japanese with English abstract)

Orsi G., De Vita S., Di Vito M., Isaia R., Nave R. & Heiken G. (2003) - *Facing volcanic and related hazards in the Neapolitan area.* Earth Sciences in Cities, **56**: 121-170.

Orsi G., Gallo G. & Zanchi A. (1991) - *Simple-shearing block resurgence in caldera depression. A model from Pantelleria and Ischia.* J. Volcanol. Geotherm. Res., **47**: 1–11.

Panzera F., D'amico S., Colica E. & Viccaro M. (2019) - *Ambient vibration measurements to support morphometric analysis of a pyroclastic cone.* Bull. Volcanol., **81** (12): 74.

Panzera F., D'amico S., Lotteri A., Galea P. & Lombardo G. (2012) - *Seismic site response of unstable steep slope using noise measurements: the case study of Xemxija Bay area, Malta.* Nat. Hazards Earth Syst. Sci., **12** (11): 3421-3431.

Pischiutta M., Salvini F., Fletcher J., Rovelli A. & Ben-Zion Y. (2012) - *Horizontal polarization of ground motion in the Hayward fault zone at Fremont, California: dominant fault-high-angle polarization and fault-induced cracks.* Geophys. J. Int., **188** (3): 1255-1272.

Poli S., Chiesa S., Gillot P.Y., Gregnanin A. & Guichard F. (1987) - *Chemistry versus time in the volcanic complex of Ischia (gulf of Naples, Italy): evidence of successive magmatic cycles.* Contrib. Mineral. Petrol., **95**: 322-335.

Rittmann A. (1930) - *Geologie der insel Ischia.* D. Reimer (E. Vohsen).

Sansivero F., De Vita S., Marotta E, Della Seta M, Martino S, Marmoni G.M. (2018) - *Field trip to the Ischia resurgent caldera, a journey across an active volcano in the Gulf of Naples.* Geological Field Trips and Maps **10** (2.2), Doi: 10.3301/GFT.2018.03.

Sbrana A. & Toccaceli R.M. (2011) - *Carta Geologica della regione Campania - Foglio 464, Isola di Ischia.* Litografia artistica cartografica, Firenze.

Selva J., Acocella V., Bisson M., Caliro S., Costa A., Della Seta M., De Martino P., De Vita S., Federico C., Giordano G., Martino S. & Cardaci C. (2019) - *Multiple natural hazards at volcanic islands: a review for the Ischia volcano (Italy).* J. Appl. Volcanol., **8** (5): 1-43.

SESAME (2004) - *Guidelines for the implementation of the H/V spectral ratio technique on ambient vibrations: measurements, processing and interpretation.* Deliverable D23.12 European Commission - Research General Directorate Project No. EVG1-CT-2000-00026 SESAME.

Strollo R., Nunziata C., Iannotta A. & Iannotta D. (2015) - *The uppermost crust structure of Ischia (southern Italy) from ambient noise Rayleigh waves.* J. Volcanol. Geotherm. Res., **297**: 39-51.

Tibaldi A. & Vezzoli L. (1998) - *The space problem of caldera resurgence: an example from Ischia Island, Italy.* Geologische Rundschau, **87**: 53-66.

Tibaldi A. & Vezzoli L. (2004) - *A new type of volcano flank failure: the resurgent caldera sector collapse, Ischia, Italy.* Geophys. Res. Lett., **31** (14): L14605.

Wathelet M., Chatelain J.-L., Cornou C., Di Giulio G., Guillier B., Ohrnberger M. & Savvaidis A. (2020) - *Geopsy: A User-Friendly Open-Source Tool Set for Ambient Vibration Processing.* Seismol. Res. Lett., **91**(3): 1878-1889.

Valentin J., Capron A., Jongmans D., Baillet L., Bottelin P., Donze F., Larose E. & Mangeney A. (2017) - *The dynamic response of prone-to-fall columns to ambient vibrations: comparison between measurements and numerical modelling.* Geophys. J. Int., **208** (2): 1058-1076.

Vezzoli L. (1988) - *Island of Ischia. In: Vezzoli L. (1988, eds),* CNR Quaderni de "La ricerca scientifica", **114** (10): 122.

Vidale J.E. (1986) - *Complex polarisation analysis of particle motion.* Bull. Seism. Soc. Am., **76**: 1393-1405.

Received September 2020 - Accepted December 2020

ANNEXES

Annex 1 - Summary of the HVSR

Code	Latitude	Longitude	Duration (min)	Instrument	Sampling Frequency (Hz)	f_0 (Hz)	Amplitude f_0	SESAME Class	f_1 (Hz)
ST_1	40.733167	13.880972	30	SARA SL06	200	0.8	4.5	B1	2.5
ST_2	40.730389	13.882972	30	SARA SL06	200	*not resonant*		B2	
ST_3	40.731639	13.885139	30	SARA SL06	200	0.7	3.5	B1	
ST_4	40.732639	13.887028	30	SARA SL06	200	7	3.5	B1	0.5
ST_5	40.731444	13.887639	30	SARA SL06	200	0.5	3	B1	
ST_5b	40.731444	13.887639	60	Lennartz LE -3D/5s	250	0.5	3	B1	
ST_6	40.730972	13.889528	30	SARA SL06	200	0.4	3.5	B1	
ST_7	40.728417	13.892583	30	SARA SL06	200	0.4	5	B1	
ST_8	40.734667	13.882056	30	SARA SL06	200	0.9	4.5	B1	2.5
ST_9	40.733806	13.878722	30	SARA SL06	200			C	
ST_9b	40.733806	13.878722	60	Lennartz LE -3D/5s	250	2.5	3.5	B1	4
ST_10	40.734056	13.878333	30	SARA SL06	200	*not resonant*		B2	
ST_10b	40.734056	13.878333	60	Lennartz LE -3D/5s	250			C	
ST_11	40.735880	13.884513	30	SARA SL06	200			C	
ST_12	40.733028	13.879083	60	Lennartz LE -3D/5s	250	0.8	3	B1	4
ST_13	40.733167	13.879083	60	Lennartz LE -3D/5s	250	0.8	3	B1	
ST_14	40.733444	13.877611	60	Lennartz LE -3D/5s	250	*not resonant*		B2	
ST_15	40.733667	13.877750	60	Lennartz LE -3D/5s	250			C	
ST_16	40.733806	13.879111	60	Lennartz LE -3D/5s	250	0.8	3	B1	
ST_17	40.733889	13.878417	60	Lennartz LE -3D/5s	250	*not resonant*		B2	
FO01S	40.739937	13.865185	60	SARA SL06	200			C	
FO02R	40.739342	13.864699	60	Lennartz LE -3D/5s	250	0.5	5	A1	
FO03S	40.735626	13.865557	60	SARA SL06	200	0.5	3	A1	6
FO04S	40.726103	13.878731	60	SARA SL06	200	*not resonant*		A2	
FO05R	40.725562	13.878643	60	Lennartz LE -3D/5s	250	*not resonant*		A2	
FO06R	40.737290	13.856242	60	Lennartz LE -3D/5s	250	0.5	5.5	A1	4
FO07S	40.730409	13.856734	60	SARA SL06	200	0.7	4	B1	6.5
FO08S	40.732031	13.867691	60	SARA SL06	200	0.5	5	B1	3
FO09R	40.731693	13.869965	60	Lennartz LE -3D/5s	250	0.5	4	A1	
FO10R	40.730830	13.857785	60	Lennartz LE -3D/5s	250	0.5	6	B1	10
FO11R	40.727512	13.861650	60	Lennartz LE -3D/5s	250	0.7	5	A1	8
FO12R	40.744293	13.870815	60	Lennartz LE -3D/5s	250	0.4	4.5	A1	
FO13R	40.720963	13.878175	60	Lennartz LE -3D/5s	250	*not resonant*		A2	
FO14R	40.719740	13.875928	60	Lennartz LE -3D/5s	250	0.4	3	B1	
FO15T	40.724250	13.864382	46	Tromino	128	0.7	3.5	B1	
FO16S	40.722427	13.865445	45	SARA SL06	200	0.8	3.5	B1	
FO17S	40.719400	13.864973	45	SARA SL06	200	1	4	B1	
FO18T	40.735954	13.868863	46	Tromino	128	0.4	3.5	B1	10
FO19S	40.738440	13.866678	45	SARA SL06	200	0.4	6	A1	
FO20S	40.721490	13.861743	45	SARA SL06	200	0.9	4	B1	
FO21S	40.721355	13.861263	38	SARA SL06	200	1	3.5	B1	7
FO22S	40.722860	13.861473	45	SARA SL06	200	0.9	6	A1	
FO23S	40.719685	13.861825	45	SARA SL06	200	1	3.5	B1	7
FO24S	40.720608	13.862510	23	SARA SL06	200	1.1	3	B1	
FO25S	40.721188	13.862572	45	SARA SL06	200	1	3.5	B1	
FO26S	40.724810	13.869987	45	SARA SL06	200	0.7	3	B1	8
FO27S	40.722590	13.867682	45	SARA SL06	200	0.8	4	B1	
FO28T	40.725497	13.878364	40	Tromino	128	*not resonant*		A2	
FO29T	40.731379	13.887567	40	Tromino	128	*not resonant*		B2	
FO30S	40.751137	13.873157	60	SARA SL06	200	4	6	A1	0.4
FO31S	40.736148	13.863751	60	SARA SL06	200	0.5	4	A1	8
FO32S	40.736121	13.861796	60	SARA SL06	200	0.5	3.5	A1	
FO33S	40.736833	13.858110	60	SARA SL06	200	0.5	5	A1	
FO34S	40.742259	13.869862	60	SARA SL06	200	0.5	5	A1	
FO35S	40.742640	13.870871	60	SARA SL06	200	0.45	3	A1	
FO36S	40.736880	13.863651	60	SARA SL06	200			C	
FO37S	40.737266	13.863422	60	SARA SL06	200	0.5	4	A1	
FO38S	40.753670	13.872624	60	SARA SL06	200	0.4	3	B1	
FO39T	40.754566	13.870226	40	Tromino	128	0.4	3	B1	4
FO40S	40.748768	13.872624	60	SARA SL06	200	0.4	3	B1	
FO41T	40.748783	13.872067	60	Tromino	128			C	
FO42S	40.745686	13.873549	36	SARA SL06	200			C	
FO43S	40.738190	13.884954	60	SARA SL06	200	*not resonant*		A2	
FO44S	40.710615	13.872682	60	SARA SL06	200	0.5	2	B1	
FO45S	40.720875	13.864524	60	SARA SL06	200	0.9	5	A1	
FO46S	40.699521	13.879019	60	SARA SL06	200			C	
FO47T	40.711164	13.875432	60	Tromino	128	0.6	3.5	B1	10
FO48S	40.716315	13.869527	60	SARA SL06	200			C	
FO101S	40.739452	13.872461	30	SARA SL06	200	0.4	3.5	A1	
FO102T	40.738136	13.872482	60	Tromino	128	0.4	3	A1	
FO103S	40.738014	13.869533	30	SARA SL06	200	0.4	5	A1	
FO104S	40.739964	13.877565	60	SARA SL06	200	*not resonant*		B2	
FO105S	40.741447	13.882757	60	SARA SL06	200	*not resonant*		A2	
FO106S	40.737915	13.868736	60	SARA SL06	200	0.4	5	A1	
FO107S	40.711823	13.860865	60	SARA SL06	200	0.6	2.5	B1	1
FO108S	40.712610	13.858859	60	SARA SL06	200			C	
FO109T	40.710213	13.855918	60	Tromino	128			C	
FO110S	40.711372	13.857001	60	SARA SL06	200	0.6	3	B1	
FO111S	40.710370	13.857049	60	SARA SL06	200	*not resonant*		B2	
FO112S	40.710674	13.856040	60	SARA SL06	200			C	
FO113T	40.712242	13.857121	60	Tromino	128	1	4	B1	

FO114S	40.711000	13.854087	60	SARA SL06	200	1	5	B1	4
FO115S	40.711920	13.856055	60	SARA SL06	200			C	
FO116T	40.709713	13.858992	60	Tromino	128			C	
FO117S	40.708477	13.857666	60	SARA SL06	200	1.5	3	B1	
FO118S	40.708885	13.858074	60	SARA SL06	200			C	
FO119S	40.707905	13.860691	60	SARA SL06	200	3.5	3	B1	1
FO120T	40.709114	13.863424	60	Tromino	128	1.5	5	B1	
FO121S	40.709873	13.868028	60	SARA SL06	200	1	2.5	B1	
FO122S	40.708744	13.864430	48	SARA SL06	200	1.5	4.5	A1	
FO123S	40.712925	13.876302	60	SARA SL06	200	0.6	3	B1	
FO124S	40.714966	13.876249	60	SARA SL06	200			C	
FO125T	40.709553	13.878666	60	Tromino	128	0.6	2.5	B1	
FO126S	40.708633	13.876716	60	SARA SL06	200	0.5	2.5	B1	
FO127S	40.709570	13.875464	60	SARA SL06	200	0.5	3.5	B1	
FO128S	40.710968	13.877057	60	SARA SL06	200	*not resonant*		B2	
FO129T	40.709250	13.876151	60	Tromino	128			C	
FO130S	40.707176	13.876628	60	SARA SL06	200	3	3	B1	0.5
FO131R	40.707785	13.877613	99	Lennartz LE -3D/5s	250	0.5	3.5	B1	0.8
FO132S	40.706990	13.872096	60	SARA SL06	200			C	
FO133T	40.705720	13.871049	60	Tromino	128	*not resonant*		B2	
FO134S	40.704903	13.874200	60	SARA SL06	200	3	4	A1	0.5
FO135S	40.704440	13.867000	60	SARA SL06	200	2.5	4	B1	
FO136S	40.707040	13.863474	60	SARA SL06	200	1.5	7	A1	
FO137S	40.703148	13.870953	60	SARA SL06	200	2	4	B1	
FO138S	40.710648	13.870879	60	SARA SL06	200			C	
FO139S	40.741932	13.865905	60	SARA SL06	200	0.4	6	A1	
FO140S	40.741592	13.864700	60	SARA SL06	200	0.4	5	B1	
FO141S	40.733680	13.856130	60	SARA SL06	200	0.5	4	A1	
FO142M	40.731865	13.855565	120			4.5	5.5	A1	
FO143T	40.746200	13.873315	60	Tromino	128	0.4	3	B1	11
FO144R	40.711826	13.870029	74	Lennartz LE -3D/5s	250	0.8	4	B1	
FO145S	40.744580	13.875870	60	SARA SL06	200			C	
FO146R	40.717450	13.867091	60	Lennartz LE -3D/5s	250	0.9	4	A1	
FO147S	40.732243	13.863508	60	SARA SL06	200	0.5	5.5	A1	12
FO148T	40.742165	13.876312	60	Tromino	128	0.5	3	B1	6.5
FO149S	40.739740	13.875821	45	SARA SL06	200	0.4	2.5	B1	
FO150R	40.704845	13.877243	73	Lennartz LE -3D/5s	250	0.5	3	B1	
FO151S	40.732067	13.864194	60	SARA SL06	200	0.5	5	A1	4
FO152R	40.702827	13.879654	60	Lennartz LE -3D/5s	250	0.5	3	B1	0.3
FO153S	40.733807	13.859359	60	SARA SL06	200	0.5	5	A1	5.5
FO154T	40.744034	13.878961	60	Tromino	128	7.7	3	B1	4.5
FO155S	40.741505	13.879818	60	SARA SL06	200	0.4	2	B1	
FO156S	40.752170	13.869139	60	SARA SL06	200	6	4	B1	0.35
FO157S	40.749107	13.868125	60	SARA SL06	200	0.4	4	B1	
FO158S	40.747784	13.867269	60	SARA SL06	200			C	
FO159S	40.745396	13.868065	60	SARA SL06	200	0.4	5	A1	
FO160S	40.747410	13.870689	54	SARA SL06	200	0.5	4.5	A1	9
FO161S	40.714775	13.865277	60	SARA SL06	200	0.8	4	B1	2.5
FO162S	40.713300	13.863047	60	SARA SL06	200	0.9	3.5	B1	0.6
FO163S	40.758194	13.871788	60	SARA SL06	200	8	4	B1	0.3
FO164R	40.757492	13.865026	60	Lennartz LE -3D/5s	250			C	
FO165T	40.716064	13.871296	50	Tromino	128	0.7	3	B1	
FO166S	40.707370	13.875943	60	SARA SL06	200	0.5	3	B1	3
FO167S	40.708965	13.866673	60	SARA SL06	200	1.7	3	B1	
FO168S	40.712400	13.856537	60	SARA SL06	200	1.2	6	A1	
FO169S	40.753395	13.880162	60	SARA SL06	200			C	
FO170S	40.750000	13.874667	60	SARA SL06	200	3.5	3	A1	
FO171S	40.755222	13.875928	60	SARA SL06	200	9	3.5	B1	0.4
FO172S	40.752598	13.877376	60	SARA SL06	200	3	3.5	B1	
FO173S	40.756990	13.873512	60	SARA SL06	200	6.7	4	B1	
FO174S	40.756710	13.874883	60	SARA SL06	200	9	3	B1	0.4

Annex 2- Correlation scheme between lithostratigraphic units proposed in literature and synthetic litotechnical units derived from the combination of lithostratigraphic units and their correlation with the interpreted survey stratigraphic data.

Map Code	Synthesis Unit	Vezzoli, 1988 (the number in bold refers to the map legend)	Sbrana & Toccaceli, 2011	Della Seta et al., 2015	Cod_New
Ad	*Man-made fill/structure*		h1 - Dumps h3 - Coastal defense works r - Anthropic structure/inactive quarry		h
Ld	*Landslide deposit*	Landslides caused by 1883 earthquake (**2**)	a1a - Landslide deposit		1
			a1b - Ancient landslide deposit	Debris slides, slump and mud flow	
Sd	*Slope debris*	Slope talus (**1**)	aa/ab Heterometric slope deposit a3 - Heterogeneous and heterometric slope debris		3
Ec	*Eluvial-colluvial deposit*	Reworked pyroclastic deposits of historical and pre-historical volcanic centers (**4**)	b2 - Eluvial and colluvial deposit	Eluvial and colluvial deposits	11
Da	*Debris avalanche*	Landslides deposits with huge blocks of Green Tuff (**40**)	PUS - "Punta del Soccorso" Unit	Debris avalanche	7
		"Scarrupo di Panza" volcanic center (**54,55**)	SUC(a,b) - "Succhivo" debris avalanche Unit		
Df	*Debris flow deposit*	Urban areas, recent beach deposits (**1**)	b - Alluvial deposit ia - Debris flow and stream flow deposits		12
			ib - Epiclastic debris and stream flow deposits		8
Mf	*Lahar (mud flow)*			Lahar debris/mud deposit	15
GrSa	*Sandy gravels and coarse marine sands, sands*	Urban areas, recent beach deposits (**1**)	g2 - Present and recent beach deposit		13
			MZV - "Mezzavia vecchia" Unit sms - Covered marine sands		4a
Cl	*Clays*			Tuffs and MEGT reworking	9
PSlo	*Stratified loose pyroclastic deposit*	"Scarrupo di Panza" volcanic center (**54,55**)	CPE - "Cava Pelara" pyroclastics PPI - "Faro Punta Imperatore" pyroclastics PPZ - "Panza" pyroclastics RUO - "Russo" pyroclastics		5a
		"Citara" Formation (**64**)	PGI - "Ciglio" pyroclastics SGL - "Sant'Angelo" tuffs TCT - "Citara" tuffs TPR - "Punta delle Pietre Rosse" tuffs		
		"Punta Imperatore" volcanic center (**79,80**)	ELF - "Elefante" pyroclastics FGN1 - "Agnone" beach pyroclastics, "Punta Imperatore" Mamber FGN2 - "Agnone" beach pyroclastics, "Pietra Nera" Mamber SRG - "Sorgeto" tuffs		
PSli	*Stratified lithoid pyroclastic deposit*	"Scarrupo di Panza" volcanic center (**54,55**)	SUN(a,b) - "Scarrupo di Panza" pyroclastics		5b
		Citara Formation (**64**)	TSPb - "Serrara-Cava Petrella" tuffs		
MEGT	*Mt. Epomeo Green Tuff (MEGT)*	Monte Epomeo Tufite (**65**) - Monte Epomeo Green Tuff (**66,68**)	BPT - "Il Porticello" breccia PBC - "Pietra Bianca" ignimbrites PZE - "Pizzone" tuff TFS - "Frassitelli" tuff TME - "Monte Epomeo" Green Tuff	Lower and Upper "Monte Epomeo" Green Tuff	5c
La	*Lavas*	"Zaro" volcanic center (**36,37**)	ZRO1 - "Zaro" lavas, "Sciavica" member ZRO2 - "Zaro" lavas, "Punta Caruso" member		6
		"Scarrupo di Panza" volcanic center (**54,55**)	POM - "Pomicione" lavas SHP - "Schiappa" splatters		
		"Pilaro" volcanic center (**56,57,58**)	GMV - "Grotta del Mavone" lavas LPR - "Pilaro" lavas RSC - "Rosicariello" lavas		
		"Monte Sant'Angelo" volcanic center (**77,78**)	LCH - "Punta Chiarito" lavas		
		"Punta Imperatore" volcanic center (**79,80**)	LCG - "Capo Negro" lavas PIM - "Punta Imperatore" lavas		
		"Rione Bocca" Lavas (**85**)	VNU - "Vagnulo" unit	Rione Bocca Trachytic Lava	